Pergamon

Int. J. Solids Structures Vol. 35, No. 11, pp. 1099–1130, 1998

0020–7683/98 $19.00 + .00

PII: S0020–7683(97)00091–7

DETAILS OF THE INTEGRAL EQUATION METHOD APPLIED TO THE ANALYSIS OF AN ADHESIVE LAYER CRACK

VICTOR GIURGIUTIU
Department of Mechanical Engineering, University of South Carolina, Columbia, SC 29208, U.S.A.

AXINTE IONITA and DAVID A. DILLARD
Department of Engineering Science and Mechanics, Virginia Polytechnic Institute and State University, Blacksburg, VA 24061-0219, U.S.A.

(*Received* 9 *March* 1997)

Abstract—The mathematical model for a crack in an elastic adhesive layer sandwiched between two adherends proposed by Fleck, Hutchinson and Suo ((1991) Crack path selection in a brittle adhesive layer. *International Journal of Solids and Structures* **27**(13), 1683–1703) was considered. The elastic mismatch between the adhesive and adherend materials modifies the far-field values of the stress intensity factors and of the T-stress in a manner that depends on the position of the crack inside the layer and on the Dundurs parameters. A complex-potential stress-function formulation, using dislocation distributions represented by truncated Chebyshev series, yielded an integral equation that was solved numerically by the method of collocations. The symbolic derivation of the integral equations was checked, and a few differences from Fleck, Hutchinson and Suo's expressions were identified and reconciled. The computational aspects of the solution were studied in detail using two programming languages, MATHCAD and C++, run on standard PC hardware. A palette of numerical techniques were utilized to study and control the consistency and accuracy of the solution. Symmetry and anti-symmetry arguments were used to identify numerically sensitive regions. Fast Fourier Transform calculation of sine and cosine Fourier integrals was used to increase speed. Convergence of intermediate and final results was examined. It was found that the method is very sensitive to the details of numerical computation, especially for combinations of parameters that lead to nearly singular matrices. © 1998 Elsevier Science Ltd.

INTRODUCTION

Cracks in adhesive layers have been observed to propagate both interfacially as well as cohesively in straight or wavy paths. Various crack propagation mechanisms have been tentatively identified. In a recent paper, Fleck *et al.* (1991) presented a modeling technique that gives numerical predictions of the stress intensity factors and T-stress at the tip of an adhesive crack as functions of the far-field stress intensity factors and T-stress and of some additive and multiplicative coefficients that depend on the elastic mismatch between the adhesive and the adherend, and on the relative position of the crack within the adhesive. The 2-material 3-region elasticity problem associated with this topic is solved by Fleck *et al.* (1991) through an integral equations method using a Chebyshev series of the unknown dislocation distribution, and several numerical techniques. We reconstructed the symbolic development and then programmed the numerical method on a standard PC. A study of the computational aspects of the method was undertaken in order to accelerate the program's performance and to keep under control the accuracy of the results. Several discrepancies with the original formulation have been noted and reconciled.

Modeling of a crack in an adhesive layer

Consider the general expression of the asymptotic stress field at the tip of a crack in an isotropic homogeneous material [Williams (1957); Westergaard (1939); Anderson (1991)]:

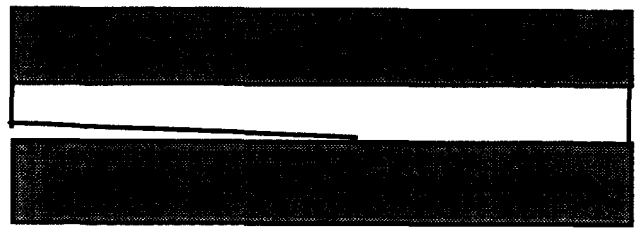

(a)

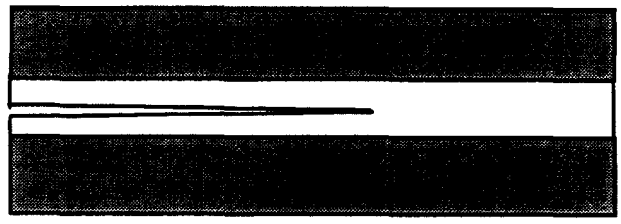

(b)

Fig. 1. Crack types in adhesive layers: (a) interfacial crack; (b) cohesive crack.

$$\begin{bmatrix} \sigma_{xx}(r,\theta) & \sigma_{xy}(r,\theta) \\ \sigma_{xy}(r,\theta) & \sigma_{yy}(r,\theta) \end{bmatrix} = \frac{K_I^\infty}{\sqrt{2\pi}} \frac{1}{\sqrt{r}} \cos\left(\frac{\theta}{2}\right) \begin{bmatrix} 1-\sin\left(\frac{\theta}{2}\right)\sin\left(\frac{3\theta}{2}\right) & \sin\left(\frac{\theta}{2}\right)\sin\left(\frac{3\theta}{2}\right) \\ \sin\left(\frac{\theta}{2}\right)\sin\left(\frac{3\theta}{2}\right) & 1+\sin\left(\frac{\theta}{2}\right)\sin\left(\frac{3\theta}{2}\right) \end{bmatrix}$$

$$+ \frac{K_{II}^\infty}{\sqrt{2\pi}} \frac{1}{\sqrt{r}} \begin{bmatrix} -\sin\left(\frac{\theta}{2}\right)\left[2+\cos\left(\frac{\theta}{2}\right)\cos\left(\frac{3\theta}{2}\right)\right] & \cos\left(\frac{\theta}{2}\right)\left[1-\sin\left(\frac{\theta}{2}\right)\sin\left(\frac{3\theta}{2}\right)\right] \\ \cos\left(\frac{\theta}{2}\right)\left[1-\sin\left(\frac{\theta}{2}\right)\sin\left(\frac{3\theta}{2}\right)\right] & \sin\left(\frac{\theta}{2}\right)\cos\left(\frac{\theta}{2}\right)\cos\left(\frac{3\theta}{2}\right) \end{bmatrix}$$

$$+ \begin{bmatrix} T & 0 \\ 0 & 0 \end{bmatrix} + O(\sqrt{r}) \quad (1)$$

where r and θ are the polar coordinates centered at the crack tip. K_I^∞ and K_{II}^∞ are the far field stress intensity factors that multiply the terms that are singular in $\sqrt{r}$. The terms which are not singular in $\sqrt{r}$ are small near the crack tip and can be neglected. The constant term T was kept in the expression though it does not have a singular behavior and it may be assumed to be small in comparison with the singular stress. The reason for retaining T lies in the fact that there is strong experimental evidence and some theoretical explanation indicating that the value of T is essential in the crack-path selection mechanism. This term is called "T-stress".

Consider a typical structural adhesive layer contained between two substrates. The adhesive and the substrate materials are assumed linear elastic, but of dissimilar elastic properties. The adhesive layer is homogeneous, and its local behavior can be assumed to be brittle. The propagation of a crack in the adhesive layer is either *interfacial*, or *cohesive* (Fig. 1). For given geometry and crack position, two separate factors influence the stress state around the crack tip: the far-field loading (stress intensity factors and T-stress), and the elastic mismatch between adhesive and adherend materials.

The far-field stress intensity factors and T-stress result from external loading and geometry of the assembly made up of the two adherends bonded together by the adhesive. The length scale of the far-field problem is much larger than the thickness of the adhesive

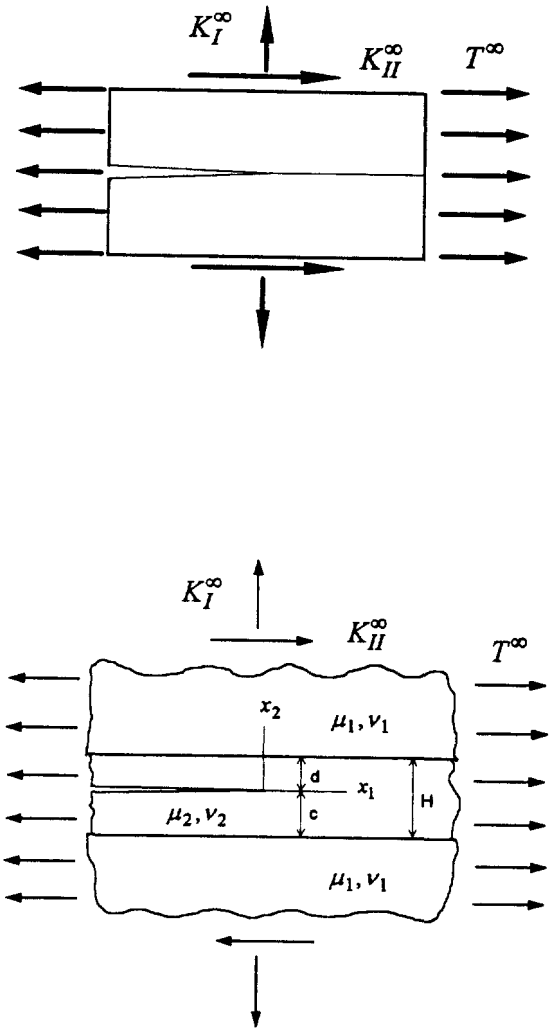

Fig. 2. Far-field and near-field effects in an adhesive joint: (a) far-field stress intensity factors, K_I^∞ and K_{II}^∞, and the T-stress result from the far-field geometry and loading (adhesive layer is neglected); (b) near-field effects are obtained by considering details of the adhesive layer, local geometry, and crack position.

layer. At this length scale (Fig. 2(a)), the influence of the adhesive layer can be neglected, and the far-field stress intensity factors, K_I^∞ and K_{II}^∞, and the T-stress result directly from classical linear fracture mechanics analysis. For simple geometries, standard fracture mechanics formulae are available (see, for example, Anderson, 1991, p. 76). For more complicated geometries, experimental analysis can be used.

The near-field model corresponds to length scales comparable with the thickness of the adhesive layer, and with the magnitude of the crack opening displacement. At this scale, the crack is modeled as a layer of finite thickness bounded by two half-planes of different elastic properties (Fig. 2(b)).

Two elastic mismatch parameters and one geometric parameter are identified. The elastic mismatch parameters (Dundurs, 1969) are:

$$\alpha = \frac{(1-\nu_2)/\mu_2 - (1-\nu_1)/\mu_1}{(1-\nu_2)/\mu_2 + (1-\nu_1)/\mu_1}, \quad \beta = \frac{1}{2}\frac{(1-2\nu_2)/\mu_2 - (1-2\nu_1)/\mu_1}{(1-\nu_2)/\mu_2 + (1-\nu_1)/\mu_1} \tag{2}$$

where μ and ν are the shear modulus and Poisson's ratio, respectively. The parameter α is related to the plane-strain Young's moduli, $\bar{E}_1$ and $\bar{E}_2$, by the relation $\alpha = (\bar{E}_1 - \bar{E}_2)/(\bar{E}_1 + \bar{E}_2)$,

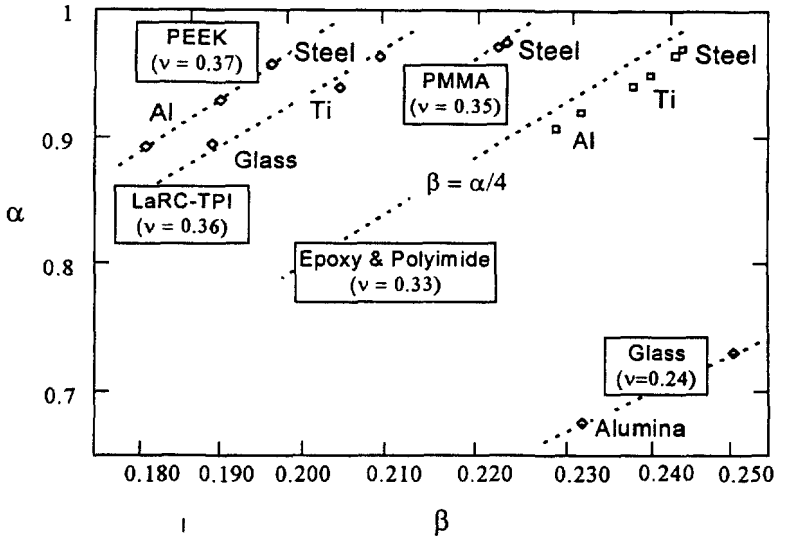

Fig. 3. Typical values of the elastic mismatch parameters for polymeric and inorganic adhesives joining various substrates. Poisson's ratio values, ν, were taken from literature, and the results are seen to be very sensitive to the actual ν of the adhesive.

where $\bar{E}_1 = 2\mu_1/(1-\nu_1)$, and $\bar{E}_2 = 2\mu_2/(1-\nu_2)$. They can also be related to the material constants, κ_1 and κ_2 as

$$\alpha = \frac{\dfrac{\kappa_2+1}{\mu_2} - \dfrac{\kappa_1+1}{\mu_1}}{\dfrac{\kappa_2+1}{\mu_2} + \dfrac{\kappa_1+1}{\mu_1}}, \quad \beta = \frac{\dfrac{\kappa_2-1}{\mu_2} - \dfrac{\kappa_1-1}{\mu_1}}{\dfrac{\kappa_2+1}{\mu_2} + \dfrac{\kappa_1+1}{\mu_1}} \tag{3}$$

where κ has the expression $\kappa = 3-4\nu$ in plane-strain problems, and $\kappa = (3-\nu)/(1+\nu)$ in plane-stress problems. Other elastic mismatch parameters that can be derived from α and β are

$$\varepsilon = \frac{1}{2\pi}\ln\frac{1-\beta}{1+\beta}, \quad \text{and} \quad \Sigma = \frac{1+\alpha}{1-\alpha}. \tag{4}$$

Typical values of the elastic mismatch parameters for common structural adhesive applications are given in Fig. 3. It can be seen that α lies between 0.88 and 0.98, while β lies between 0.175 and 0.255. The relationship between α and β follows a straight line with the slope depending on the Poisson ratio value. For $\nu = 1/3$, the slope of this curve is 1/4, i.e. $\alpha = 4\beta$. In our numerical tests, we took the epoxy/aluminum adhesive/adherend pair with $\mu_1 = 26.3$ GPa, $\nu_1 = 0.35$, $\mu_2 = 1.5$ GPa, $\nu_2 = 0.34$, and hence, $\alpha = 0.893$ and $\beta = 0.217$.

The geometric parameter of the problem is the crack placement ratio c/H. For $c/H = 0.5$, the problem is symmetrical and mode I far-field loading will induce mode I near-field stresses only. As c/H approaches either 0 or 1, the problem becomes more and more asymmetric, and a mode I far field loading will induce both mode I and mode II local field stresses. Another geometric parameter that appears in this problem is d/H. This parameter is not independent, but it is related to c/H through the formula $d/H = 1-c/H$.

The far-field stress intensity factors, K_I^∞ and K_{II}^∞, and the far field T-stress, T^∞, represent the loading for the near-field problem. Due to the interaction between the adhesive layer and the dissimilar adherends, the near-field stress intensity factors, K_I and K_{II}, and the near field T-stress, T, are different from the far field values.

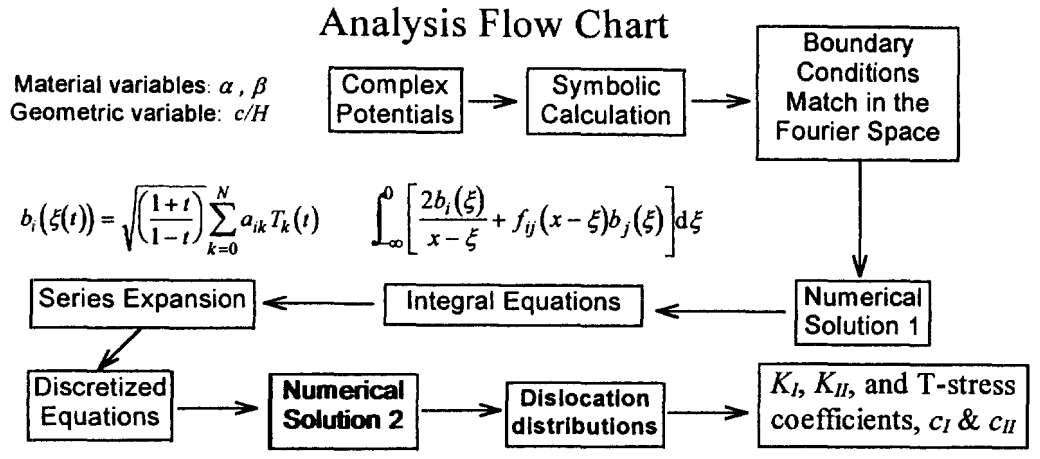

Fig. 4. Analysis flow chart for the integral equation method applied to the linear fracture mechanics analysis of an adhesive layer crack.

Problem outline

The problem consists of finding the relationship between the far-field stress intensity factors and T-stress, and the local stress intensity factors and T-stress, for various combinations of elastic and geometric parameters of the adhesive/adherend pair. This relationship can be established numerically by solving the elasticity problem represented in Fig. 2(b). The analytical method used to solve the problem is that of integral equations. The crack is modeled with an unknown distribution of dislocations. Analytical expressions are developed for the stress an displacement fields due to a single dislocation in a layered material system. The combined effect of the entire distribution of dislocations is expressed through a system of integral equations. The zero-traction condition on the crack face, and the K_I^{∞}, K_{II}^{∞} values in the far field, are imposed. To obtain numerical solutions, the distribution of dislocations is represented in a truncated Chebyshev series of order N, and the system of integral equations is evaluated at the same number, N, of collocation points. Solution of the resulting linear algebraic system yields the unknown Chebyshev coefficients, and reassembly of the series expansion recovers the distribution of dislocations. Using the distribution of dislocations, the local stress and displacement fields, stress-intensity factors, and T-stress can be calculated. A schematic of the solution process is presented in Fig. 4.

PRELIMINARY ELASTICITY RESULTS

The problem of a crack in an adhesive layer is best described using two-dimensional plane-strain elasticity in stress function formulation. For convenience, both the Airy stress function and Muskhelisvili's complex potentials are used. The bi-material interface conditions play a crucial role and are discussed separately.

Airy stress function formulation for plane elasticity problems

The Airy stress function formulation is developed in terms of Airy function, $U(x, y)$, and the companion function, $X(x, y)$. The functions U and X satisfy the differential equations

$$\nabla^4 U = 0 \quad \text{and} \quad \nabla^2 X = 0, \tag{5}$$

and are connected by the differential equation:

$$\frac{\partial^2 X}{\partial x\,\partial y} = \frac{1}{4}\nabla^2 U. \tag{6}$$

The stresses are given by

$$\sigma_{xx} = \frac{\partial^2 U}{\partial y^2}, \quad \sigma_{yy} = \frac{\partial^2 U}{\partial x^2}, \quad \sigma_{xy} = -\frac{\partial^2 U}{\partial x\,\partial y}, \tag{7}$$

and the displacements are given by

$$2\mu u = -\frac{\partial U}{\partial x} + (\kappa+1)\frac{\partial X}{\partial y}, \quad 2\mu v = -\frac{\partial U}{\partial y} + (\kappa+1)\frac{\partial X}{\partial x}. \tag{8}$$

The displacement gradient with respect to x is given by

$$\frac{\partial u}{\partial x} = -\frac{1}{2\mu}\frac{\partial^2 U}{\partial x^2} + \frac{\kappa+1}{2\mu}\frac{\partial^2 X}{\partial x\,\partial y}, \quad \frac{\partial v}{\partial x} = -\frac{1}{2\mu}\frac{\partial^2 U}{\partial x\,\partial y} + \frac{\kappa+1}{2\mu}\frac{\partial^2 X}{\partial x^2}. \tag{9}$$

The material constant, κ, has the expression $\kappa = 3-4\nu$ in the plane-strain problems, and $\kappa = (3-\nu)/(1+\nu)$ in plane-stress problems.

Muskhelisvili's complex potentials formulation for plane elasticity problems

Using the complex variable $z = x+iy$, Muskhelisvili's (1963) writes:

$$\sigma_{xx} + \sigma_{yy} = 2[\Phi(z) + \bar{\Phi}(\bar{z})] \tag{10}$$

$$\sigma_{yy} - \sigma_{xx} + 2i\sigma_{xy} = 2[\bar{z}\Phi'(z) + \Psi(z)] \tag{11}$$

$$2\mu(u+iv) = \kappa\varphi(z) - z\bar{\varphi}(\bar{z}) - \bar{\psi}(\bar{z}) \tag{12}$$

where $\Phi(z) = \varphi'(z)$, $\Psi(z) = \psi'(z)$. Adding eqns (10) and (11), and taking the complex conjugate of the results yields

$$\sigma_{yy} - i\sigma_{xy} = [\Phi(z) + \bar{\Phi}(\bar{z}) + z\bar{\Phi}'(\bar{z}) + \bar{\Psi}(\bar{z})]. \tag{13}$$

It is convenient to introduce the auxiliary function

$$\Omega(z) = -\bar{\Phi}(z) - z\bar{\Phi}'(z) - \bar{\Psi}(z), \tag{14a}$$

and its conjugate

$$\Psi(z) = -\bar{\Omega}(z) - \Phi(z) - z\Phi'(z). \tag{14b}$$

Using eqns (14a) and (14b) in eqn (13) yields the complex stress expression

$$\sigma_{yy} - i\sigma_{xy} = [\Phi(z) - \Omega(\bar{z}) + (z-\bar{z})\bar{\Phi}'(\bar{z})]. \tag{15}$$

Similarly, one gets the displacements expression

$$2\mu(u+iv) = \kappa\varphi(z) + w(\bar{z}) - (z-\bar{z})\bar{\Phi}(\bar{z}) + \text{const}, \quad \text{where } w(z) = \int\bar{\Omega}(z). \tag{16}$$

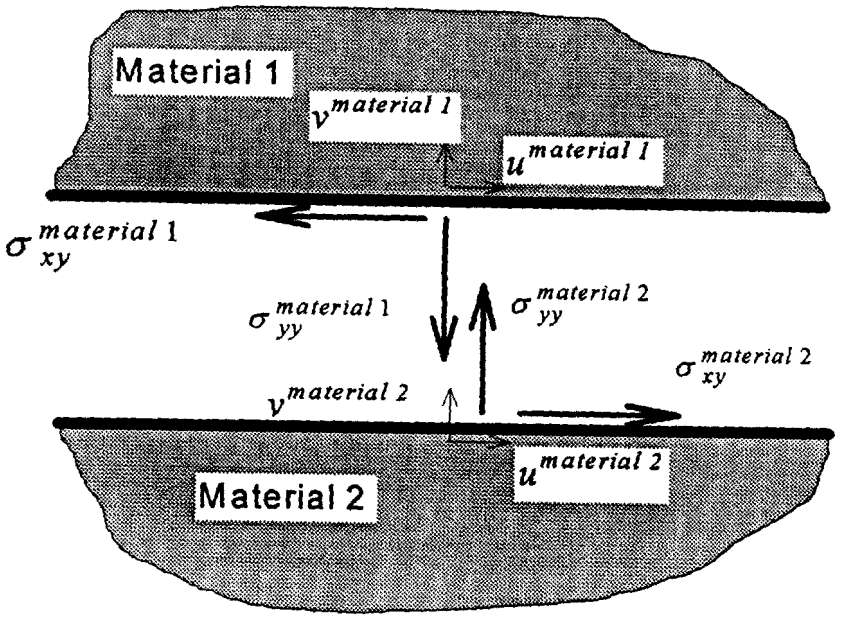

Fig. 5. The bi-material interface conditions.

In the boundary matching problems, the displacements are more conveniently expressed in differential form, thus avoiding the integration constants associated with rigid-body motions. Differentiating eqn (16) with respect to x, and dividing by 2μ yields the expression of the displacement gradient:

$$\left(\frac{\partial u}{\partial x}+i\frac{\partial v}{\partial x}\right)=\frac{\kappa}{2\mu}\Phi(z)+\frac{1}{2\mu}[(\bar{z}-z)\overline{\Phi'(z)}-\Phi(\bar{z})]. \tag{17}$$

Muskhelisvili's complex potentials formulation can be related to the Airy stress function formulation. Thus, the functions $\varphi(z)$ and $\psi(z)$ can be used to calculate the Airy function (Muskhelisvili, 1963):

$$U(x,y)=\mathscr{R}e[\bar{z}\phi(z)+\int\psi(z)\,dz]. \tag{18}$$

The bi-material interface conditions

Consider a bi-material interface between material 1 and material 2. Traction equilibrium and displacement compatibility must be satisfied.

Traction equilibrium conditions. The traction equilibrium conditions can be expressed as:

$$\begin{aligned}(p_x)^{\text{material 1}}+(p_x)^{\text{material 2}}&=0,\\(p_y)^{\text{material 1}}+(p_y)^{\text{material 2}}&=0\end{aligned} \tag{19}$$

where p_x and p_y are the tractions in the x and y directions, respectively.

For a general curvilinear interface, the tractions p_x and p_y are defined using the components n_x and n_y of the external normal, $\vec{n}$, and hence

$$\begin{aligned}(\sigma_{xx}n_x+\sigma_{xy}n_y)^{\text{material 1}}+(\sigma_{xx}n_x+\sigma_{xy}n_y)^{\text{material 2}}&=0,\\(\sigma_{xy}n_x+\sigma_{yy}n_y)^{\text{material 1}}+(\sigma_{xy}n_x+\sigma_{yy}n_y)^{\text{material 2}}&=0.\end{aligned} \tag{20}$$

In our case (Fig. 5), $n_x=0$, $n_y=-1$, for material 1, and $n_x=0$, $n_y=1$, for material 2. Hence eqn (20) becomes

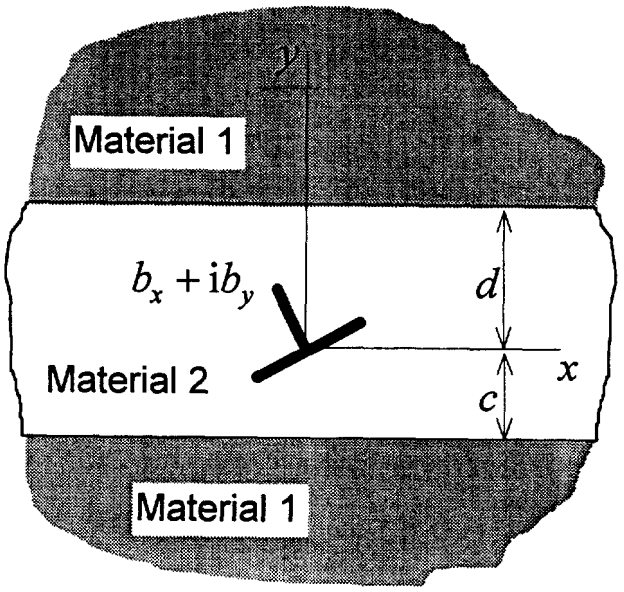

Fig. 6. An edge dislocation in a three-layer material system.

$$-\sigma_{xy}^{\text{material 1}} + \sigma_{xy}^{\text{material 2}} = 0,$$
$$-\sigma_{yy}^{\text{material 1}} + \sigma_{yy}^{\text{material 2}} = 0. \tag{21}$$

Displacement compatibility conditions.

$$(u)^{\text{material 1}} = (u)^{\text{material 2}},$$
$$(v)^{\text{material 1}} = (v)^{\text{material 2}}. \tag{22}$$

To avoid the effects of rigid body rotations, displacement continuity can be conveniently expressed in terms of the displacement gradient along the interface using eqn (17).

Displacement gradient jump in terms of Muskhelisvili's complex potentials. If one attempts to use the same stress function or Muskhelisvili's complex potentials across a bi-material interface, a certain displacement discontinuity will result. For example, one can use eqn (17) to evaluate the displacement gradient above and below the bi-material interface by using the same complex potential $\Phi(z)$, and changing only the material constants μ and κ. Upon subtraction, one gets the displacement gradient jump

$$\left(\Delta\frac{\partial u}{\partial x} + i\Delta\frac{\partial v}{\partial x}\right)^{\text{dislocation}} = \left(\frac{\partial u}{\partial x} + i\frac{\partial v}{\partial x}\right)^{\text{material 1}} - \left(\frac{\partial u}{\partial x} + i\frac{\partial v}{\partial x}\right)^{\text{material 2}}$$
$$= \frac{2\mu_2}{\kappa_2+1}\left(\frac{\kappa_1}{2\mu_1} - \frac{\kappa_2}{2\mu_2}\right)\Phi(z) + \left(\frac{1}{2\mu_1} - \frac{1}{2\mu_2}\right)[(\bar{z}-z)\overline{\Phi'(z)} - \Phi(\bar{z})]. \tag{23}$$

Multiplying both sides of eqn (23) by $2\mu_2/(\kappa_2+1)$ yields a non-dimensional expression of the displacement gradient jump in terms of Dundurs' parameters, i.e.,

$$\frac{2\mu_2}{\kappa_2+1}\left(\Delta\frac{\partial u}{\partial x} + i\Delta\frac{\partial v}{\partial x}\right)^{\text{dislocation}} = -\left(\frac{\alpha+\beta}{1+\alpha}\right)\Phi(z) - \left(\frac{\alpha-\beta}{1+\alpha}\right)[(\bar{z}-z)\overline{\Phi'(z)} - \Phi(\bar{z})]. \tag{24}$$

EDGE DISLOCATION IN A LAYERED MATERIAL SYSTEM

Consider the problem of an edge dislocation in a layered material system (Fig. 6). The dislocation of strength $b_x + ib_y$ is placed inside the middle layer (material 2), at distance d

from the upper interface, and distance c from the lower interface. The origin 0 of the x–y system of axes is taken at the dislocation. We tackle this problem through the superposition of two simpler problems:

- Problem 1: Determine the stress and displacement fields due to an edge dislocation placed at the origin of an infinite homogenous elastic plane.
- Problem 2: Determine the correction stress and displacement fields needed to compensate for displacement discontinuities at the bi-material interfaces.

Problem 1 develops the complex potential for calculating the stress and displacement fields due to a dislocation placed in a homogeneous plane, e.g. the middle layer. If we use the same complex potential in the outer layers, displacement discontinuities will be registered at the bi-material interfaces. To compensate for these displacement discontinuities, one uses the corrections generated by Problem 2. Thus, the stress and displacement fields for the complete problem result from the linear superposition of the stress and displacement fields of Problem 1 and Problem 2.

Problem 1: edge dislocation in a homogenous infinite plane

An edge dislocation in a homogenous infinite plane introduces a non-uniformity of displacements defined by Burger's vectors b_x and b_y. It can be shown (Suo, 1990; Ionita *et al.*, 1996) that Muskhelisvili's complex potentials for an edge dislocation of complex Burger's vector b_x+ib_y placed at the origin of the complex plane are:

$$\Phi(z) = \frac{\mu(b_y - ib_x)}{\pi(\kappa+1)}\frac{1}{z} = \frac{A}{z}, \tag{25}$$

$$\Omega(z) = -\frac{\mu(b_y - ib_x)}{\pi(\kappa+1)}\frac{1}{z} = -\frac{A}{z} \tag{26}$$

where $A = \mu(b_y - ib_x)/\pi(\kappa+1)$. Using eqns (25) and (26) in eqn (14b) yields the expression for $\Psi(z)$

$$\Psi(z) = \frac{\mu(b_y + ib_x)}{\pi(\kappa+1)}\frac{1}{z} = \frac{\bar{A}}{z}. \tag{27}$$

Integrating eqns (25) and (27) yields $\varphi(z) = A\ln z$, and $\psi(z) = \bar{A}\ln z$. Using eqn (18) yields

$$U(x,y) = \frac{2\mu}{(\kappa+1)\pi}(b_y x - b_x y)\ln r, \quad r = \sqrt{x^2+y^2}. \tag{28}$$

Substituting eqn (28) into eqn (7) yields the stress expressions:

$$\begin{aligned}
\sigma_{xx} &= \frac{\mu}{(\kappa+1)\pi}\left[-2b_x\left(\frac{y}{r^2}+\frac{2x^2y}{r^4}\right)+2b_y\left(\frac{x}{r^2}-\frac{2xy^2}{r^4}\right)\right],\\
\sigma_{yy} &= \frac{\mu}{(\kappa+1)\pi}\left[2b_x\left(-\frac{y}{r^2}+\frac{2x^2y}{r^4}\right)+2b_y\left(\frac{x}{r^2}+\frac{2xy^2}{r^4}\right)\right],\\
\sigma_{xy} &= \frac{\mu}{(\kappa+1)\pi}\left[2b_x\left(\frac{y}{r^2}-\frac{2xy^2}{r^4}\right)+2b_y\left(-\frac{y}{r^2}+\frac{2x^2y}{r^4}\right)\right].
\end{aligned} \tag{29}$$

Displacements discontinuity induced by the dislocation field at the material interface

For a dislocation placed in the middle layer, the complex potentials expressions given by eqns (25) and (26) are defined using the properties of material 2. As we attempt to use

the same complex potentials outside the middle layer, i.e. in material 1 regions, a finite displacement discontinuity will be registered at the bi-material interface. Using eqn (25) into eqn (24) yields the displacement gradient jump at the bi-material interface, due to a dislocation of strength $b_x + ib_y$ placed in the material 2 layer:

$$\frac{2\mu_2}{\kappa_2+1}\left(\Delta\frac{\partial u}{\partial x}+i\Delta\frac{\partial v}{\partial x}\right)^{\text{dislocation}} = -\left(\frac{\alpha+\beta}{1+\alpha}\right)\frac{A}{z}-\left(\frac{\alpha-\beta}{1+\alpha}\right)\left(2iy\frac{\bar{A}}{\bar{z}^2}-\frac{A}{\bar{z}}\right), \tag{30}$$

where $A = \mu_2(b_y - ib_x)/\pi(\kappa_2+1)$. The real part of eqn (30) yields the u-component of the displacement gradient jump, i.e.:

$$\left(\Delta\frac{\partial u}{\partial x}\right)^{\text{dislocation}} = b_x\left(\Delta\frac{\partial u}{\partial x}\right)_{b_x}^{\text{dislocation}} + b_y\left(\Delta\frac{\partial u}{\partial x}\right)_{b_y}^{\text{dislocation}}, \tag{31}$$

where $(\Delta(\partial u/\partial x))_{b_x}^{\text{dislocation}}$ and $(\Delta(\partial u/\partial x))_{b_y}^{\text{dislocation}}$ are influence coefficients due to Burger's vectors b_x and b_y respectively, i.e.,

$$\left(\Delta\frac{\partial u}{\partial x}\right)_{b_x}^{\text{dislocation}} = \frac{1}{\pi(1+\alpha)}\left[(2\alpha-\beta)\frac{y}{r^2}-2(\alpha-\beta)\frac{y^3}{r^4}\right], \tag{32}$$

$$\left(\Delta\frac{\partial u}{\partial x}\right)_{b_y}^{\text{dislocation}} = \frac{1}{\pi(1+\alpha)}\left[-\beta\frac{x}{r^2}+2(\alpha-\beta)\frac{xy^2}{r^4}\right]. \tag{33}$$

Similarly, the imaginary part of eqn (30) yields the v-components of the displacement gradient jump, i.e.,

$$\left(\Delta\frac{\partial v}{\partial x}\right)^{\text{dislocation}} = b_x\left(\Delta\frac{\partial v}{\partial x}\right)_{b_y}^{\text{dislocation}} + b_y\left(\Delta\frac{\partial v}{\partial x}\right)_{b_y}^{\text{dislocation}} \tag{34}$$

where

$$\left(\Delta\frac{\partial v}{\partial x}\right)_{b_x}^{\text{dislocation}} = \frac{1}{\pi(1+\alpha)}\left[\beta\frac{x}{r^2}+2(\alpha-\beta)\frac{xy^2}{r^4}\right], \tag{35}$$

$$\left(\Delta\frac{\partial v}{\partial x}\right)_{b_y}^{\text{dislocation}} = \frac{1}{\pi(1+\alpha)}\left[\beta\frac{y}{r^2}+2(\alpha-\beta)\frac{y^3}{r^4}\right]. \tag{36}$$

Problem 2: correction stress fields

Problem 2 cancels the displacement gradient jump induced by Problem 1. To this effect, consider the problem of a three-layer two-material system having stress-free infinite boundaries and prescribed displacement gradient jumps at the bi-material interfaces, equal in magnitude and of opposite signs to those given by eqns (31)–(36). Problem 2 will be treated with the Airy stress function formulation as given by eqns (3)–(8). By matching the free-boundary conditions in the far field and by satisfying the traction equilibrium and displacement gradient jump at the interface, we are going to determine the Airy stress function, $U(x, y)$, and its companion function, $X(x, y)$. The Fourier transform with respect to the variable x is used. To keep the formulation manageable, the effects of b_x and b_y are considered separately, and the effect of the *odd* and *even* behavior in the variable x of the displacement gradients, $\partial u/\partial x$ and $\partial v/\partial x$, and of the functions, $U(x, y)$ and $X(x, y)$, is used.

Correction stress field for b_x

Assume $b_x = 1$, and $b_y = 0$. According to eqns (32) and (35), the displacement gradient $(\partial u/\partial x)_{b_x}$ is even in the variable x, while $(\partial v/\partial x)_{b_x}$ is odd. Examination of eqns (7) and (9) yields that $U(x, y)$ must be even in x, while $X(x, y)$ must be odd. Hence, we use the appropriate Fourier sine and cosine transforms, i.e.

$$\mathscr{F}_c(U(x,y)) = \tilde{U}(\lambda, y) = \frac{2}{\pi}\int_0^\infty U(x,y)\cos\lambda x\,\mathrm{d}x$$

$$\mathscr{F}_s(X(x,y)) = \tilde{X}(\lambda, y) = \frac{2}{\pi}\int_0^\infty X(x,y)\sin\lambda x\,\mathrm{d}x.$$

Applying the Fourier transform to eqn (5), yields

$$\mathscr{F}_c(\nabla^4 U) = \lambda^4\tilde{U} - 2\lambda^2\frac{\partial^2\tilde{U}}{\partial y^2} + \frac{\partial^4\tilde{U}}{\partial y^4} = 0.$$

The roots of the characteristic equation are given by

$$(r-\lambda)^2(r+\lambda)^2 = 0 \Rightarrow \begin{cases} r_{1,2} = -\lambda \\ r_{3,4} = \lambda \end{cases},$$

and the general solution is

$$\tilde{U}(\lambda, y) = \left(\frac{A_1}{\lambda^2} + \frac{A_2}{\lambda}y\right)e^{-\lambda y} + \left(\frac{A_3}{\lambda^2} + \frac{A_4}{\lambda}y\right)e^{\lambda y}, \tag{37}$$

where the coefficients $A_1, \ldots, A_4$ may be functions of λ. Applying the inverse cosine transform yields the physical-domain expression

$$U(x,y) = \int_0^\infty \left[\left(\frac{A_1}{\lambda^2} + \frac{A_2}{\lambda}y\right)e^{-\lambda y} + \left(\frac{A_3}{\lambda^2} + \frac{A_4}{\lambda}y\right)e^{\lambda y}\right]\cos\lambda x\,\mathrm{d}\lambda. \tag{38}$$

Substituting eqn (37) into the Fourier transform of eqn (6) yields

$$\tilde{X}(\lambda, y) = \frac{1}{2\lambda^2}(A_2\,e^{-\lambda y} + A_4\,e^{\lambda y}). \tag{39}$$

Integrating with respect to y, and performing the inverse Fourier transform yields:

$$X(x,y) = \int_0^\infty \frac{1}{2\lambda^2}(A_2\,e^{-\lambda y} + A_4\,e^{\lambda y})\sin\lambda x\,\mathrm{d}\lambda. \tag{40}$$

Substitution of eqns (37) and (40) into the Fourier transform of eqn (7) yields the expression of stresses in the Fourier domain:

$$\tilde{\sigma}_{yy} = \mathscr{F}_c(\sigma_y) = -\lambda^2\tilde{U}, \quad \tilde{\sigma}_{xy} = \mathscr{F}_s(\sigma_{xy}) = \lambda\frac{\partial\tilde{U}}{\partial y}$$

i.e.,

$$\tilde{\sigma}_{yy} = (-A_1 - A_2\lambda y)\, e^{-\lambda y} + (-A_3 - A_4\lambda y)\, e^{\lambda y} \tag{41}$$

$$\tilde{\sigma}_{xy} = [-A_1 + (1-\lambda y)A_2]\, e^{-\lambda y} + [A_3(1+\lambda y)A_4]\, e^{\lambda y}. \tag{42}$$

Substitution of eqns (37) and (40) into the Fourier transform of eqn (9) yields the expression of displacement gradients in the Fourier domain:

$$\frac{\partial \tilde{u}}{\partial x} = \mathscr{F}_c\left(\frac{\partial u}{\partial x}\right) = \frac{1}{2\mu}\lambda^2 \tilde{U} + \frac{\kappa+1}{2\mu}\lambda\frac{\partial \tilde{X}}{\partial y},$$

$$= \frac{1}{2\mu}[(A_1 + A_2\lambda y)\, e^{-\lambda y} + (A_3 + A_4\lambda y)\, e^{\lambda y}] + \frac{b_x}{2}\left(\frac{\kappa+1}{2\mu}\right)(-A_2\, e^{-\lambda y} + A_4\, e^{\lambda y}), \tag{43}$$

$$\frac{\partial \tilde{v}}{\partial x} = \mathscr{F}_s\left(\frac{\partial v}{\partial x}\right) = \frac{1}{2\mu}\lambda\frac{\partial \tilde{U}}{\partial y} - \frac{\kappa+1}{2\mu}\lambda^2 \tilde{X}$$

$$= \frac{1}{2\mu}\{[-A_1 + (1-\lambda y)A_2]\, e^{-\lambda y} + [A_3 + (1+\lambda y)A_4)]\, e^{\lambda y}\}$$

$$- \frac{b_x}{2}\left(\frac{\kappa+1}{2\mu}\right)(A_2\, e^{-\lambda y} + A_4\, e^{\lambda y}). \tag{44}$$

Upon simplification

$$2\frac{\partial \tilde{u}}{\partial x} = \frac{1}{\mu}\left(A_1 + A_2\lambda y - \frac{\kappa+1}{2}A_2\right)e^{-\lambda y} + \left(A_3 + A_4\lambda y + \frac{\kappa+1}{2}A_4\right)e^{\lambda y}, \tag{45}$$

$$2\frac{\partial \tilde{v}}{\partial x} = \frac{1}{\mu}\left(A_2 + A_1 - A_2\lambda y - \frac{\kappa+1}{2}A_2\right)e^{-\lambda y} + \left(A_3 + A_4 + A_4\lambda y - \frac{\kappa+1}{2}A_4\right)e^{\lambda y}. \tag{46}$$

Expressions for the functions U *and* X *in each layer.* It can be seen that 4 coefficients, A_1, A_2, A_3, and A_4, determine fully the potentials $U(x, y)$ and $X(x, y)$ in a material region. In our three-region model, a total of 12 coefficients need to be determined from the boundary conditions applicable to each region. We designate these A_i coefficients as C_i in layer 1, D_i in layer 2, and E_i in layer 3. The outer regions (layers 1 and 3, made of material 1) are semi-infinite, and their far-field boundary is free of stresses and displacement gradients.

Hence, the functions U and X must vanish at $y \to \pm\infty$ together with all their derivatives. This implies that $C_3 = C_4 = 0$ in layer 1, and $E_1 = E_2 = 0$, in layer 3. Thus, the following functions are used:
In layer 1 $(d < y)$:

$$\tilde{U}(\lambda, y) = b_x\left(\frac{C_1}{\lambda^2} + \frac{C_2}{\lambda}y\right)e^{-\lambda y}, \quad \tilde{X}(\lambda, y) = b_x\frac{C_2}{2\lambda^2}e^{-\lambda y}$$

$$U(x, y) = b_x\int_0^\infty \left(\frac{C_1}{\lambda^2} + \frac{C_2}{\lambda}y\right)e^{-\lambda y}\cos\lambda x\, \mathrm{d}\lambda, \quad X(x, y) = b_x\int_0^\infty \frac{C_2}{2\lambda^2}e^{-\lambda y}\sin\lambda x\, \mathrm{d}\lambda. \tag{47}$$

In layer 2 ($-c < y < d$):

$$\tilde{U}(\lambda, y) = b_x \left[\left(\frac{D_1}{\lambda^2} + \frac{D_2}{\lambda} y \right) e^{-\lambda y} + \left(\frac{D_3}{\lambda^2} + \frac{D_4}{\lambda} y \right) e^{\lambda y} \right], \quad \tilde{X}(\lambda, y) = b_x \frac{1}{2\lambda^2} (D_2 e^{-\lambda y} + D_4 e^{\lambda y})$$

$$U(x, y) = b_x \int_0^\infty \left[\left(\frac{D_1}{\lambda^2} + \frac{D_2}{\lambda} y \right) e^{-\lambda y} + \left(\frac{D_3}{\lambda^2} + \frac{D_4}{\lambda} y \right) e^{\lambda y} \right] \cos \lambda x \, d\lambda,$$

$$X(x, y) = b_x \int_0^\infty \frac{1}{2\lambda^2} (D_2 e^{-\lambda y} + D_4 e^{\lambda y}) \sin \lambda x \, d\lambda. \tag{48}$$

In layer 3 ($y < -c$):

$$\tilde{U}(\lambda, y) = b_x \left(\frac{E_3}{\lambda^2} + \frac{E_4}{\lambda} y \right) e^{-\lambda y}, \quad \tilde{X}(\lambda, y) = b_x \frac{E_4}{2\lambda^2} e^{\lambda y}$$

$$U(x, y) = b_x \int_0^\infty \left(\frac{E_3}{\lambda^2} + \frac{E_4}{\lambda} y \right) e^{\lambda y} \cos \lambda x \, d\lambda, \quad X(x, y) = b_x \int_0^\infty \frac{E_4}{2\lambda^2} e^{\lambda y} \sin \lambda x \, d\lambda. \tag{49}$$

Note that the 8 unknown constants, C_1, C_2, D_1, D_2, D_3, D_4, E_3, E_4 must be determined from the bi-material interface conditions.

Bi-material interface conditions in the Fourier domain. The traction equilibrium and displacement compatibility conditions expressed by eqns (21) and (22) are transformed into the Fourier domain. Thus, eqn (21) becomes

$$\begin{aligned} (\tilde{\sigma}_{xy})^{\text{material 1}} &= (\tilde{\sigma}_{xy})^{\text{material 2}}, \\ (\tilde{\sigma}_{yy})^{\text{material 1}} &= (\tilde{\sigma}_{yy})^{\text{material 2}}, \end{aligned} \tag{50}$$

where the *tilde* symbol designates the Fourier transform. The displacement gradient jump due to the correction field must be equal and of opposite sign with the displacement gradient jump due to the dislocation field. Hence

$$\begin{aligned} \left(\Delta \frac{\partial \tilde{u}}{\partial x} \right) &= -\left(\Delta \frac{\partial \tilde{u}}{\partial x} \right)^{\text{dislocation}} \\ \left(\Delta \frac{\partial \tilde{v}}{\partial x} \right) &= -\left(\Delta \frac{\partial \tilde{v}}{\partial x} \right)^{\text{dislocation}} \end{aligned} \tag{51}$$

where the superscript *dislocation* refers to the expressions given in eqns (32) and (35) for $b_x = 1$, and $b_y = 0$. By applying eqns (50) and (51) in turn at $y = d$ and $y = -c$ interfaces, we obtain the 8 equations necessary for the determination of the unknown constants C_1, C_2, D_1, D_2, D_3, D_4, E_3, E_4.

Interface Conditions at y = d. At interface $y = d$, the upper layer corresponds to material 1 and the lower layer to material 2. Substituting eqns (41) and (42) into eqn (50), and using coefficients C_1, C_2 above the interface and D_1, D_2, D_3, D_4, below the interface, yields

$$(C_1 - C_2 + \lambda d C_2) e^{-\lambda d} + (-D_1 + D_2 - \lambda d D_2) e^{-\lambda d} + (D_3 + D_4 + \lambda d D_4) e^{\lambda d} = 0 \tag{52}$$

$$(C_1 + \lambda d C_2) e^{-\lambda d} + (-D_1 - \lambda d D_2) e^{-\lambda d} + (-D_3 - \lambda d D_4) e^{\lambda d} = 0. \tag{53}$$

Similarly, substituting eqns (45) and (46) into eqn (51) yields

$$\frac{1}{\mu_1}\left(C_1+\lambda d C_2-\frac{\kappa_1+1}{2}C_2\right)e^{-\lambda d}-\frac{1}{\mu_2}\left(D_1+\lambda d D_2-\frac{\kappa_2+1}{2}\right)e^{-\lambda d}$$
$$-\frac{1}{\mu_2}\left(D_3+\lambda d D_4+\frac{\kappa_2+1}{2}\right)e^{\lambda d}=-2\left(\Delta\frac{\partial\tilde{u}}{\partial x}\right)_{b_x}^{\text{dislocation}}, \quad (54)$$

$$\frac{1}{\mu_1}\left(C_2-C_1-\lambda d C_2-\frac{\kappa_1+1}{2}C_2\right)e^{-\lambda d}-\frac{1}{\mu_2}\left(D_2-D_1-\lambda d D_2-\frac{\kappa_2+1}{2}\right)e^{-\lambda d}$$
$$-\frac{1}{\mu_2}\left(D_3+D_4+\lambda d D_4+\frac{\kappa_2+1}{2}\right)e^{\lambda d}=-2\left(\Delta\frac{\partial\tilde{v}}{\partial x}(\lambda,d)\right)_{b_x}^{\text{dislocation}}. \quad (55)$$

Dividing eqn (52) by μ_1 and adding to eqn (55) gives

$$-\frac{\kappa_1+1}{2\mu_1}C_2\,e^{-\lambda d}+\left(\frac{1}{\mu_2}-\frac{1}{\mu_1}\right)D_1\,e^{-\lambda d}-\left(\frac{1}{\mu_2}-\frac{1}{\mu_1}\right)(1-\lambda d)D_2\,e^{-\lambda d}$$
$$+\frac{\kappa_2+1}{2\mu_2}D_2\,e^{-\lambda d}-\left(\frac{1}{\mu_2}-\frac{1}{\mu_1}\right)D_3\,e^{\lambda d}-\left(\frac{1}{\mu_2}-\frac{1}{\mu_1}\right)(1+\lambda d)D_4\,e^{\lambda d}$$
$$+\frac{\kappa_2+1}{2\mu_2}D_4\,e^{\lambda d}=-\frac{2\mu_2}{\kappa_2+1}\Sigma\left(\Delta\frac{\partial v}{\partial x}(\lambda,d)\right)_{b_x}^{\text{dislocation}}.$$

Using the non-dimensional parameters α, β and Σ of eqns (3) and (4) yields

$$\left(\frac{\alpha-\beta}{1-\alpha}\right)D_1\,e^{-\lambda d}+\left[-\left(\frac{\alpha-\beta}{1-\alpha}\right)(1-\lambda d)+\frac{\Sigma}{2}\right]D_2\,e^{-\lambda d}-\left(\frac{\alpha-\beta}{1-\alpha}\right)D_3\,e^{\lambda d}$$
$$+\left[-\left(\frac{\alpha-\beta}{1-\alpha}\right)(1+\lambda d)+\frac{\Sigma}{2}\right]D_4\,e^{\lambda d}-\frac{1}{2}C_2\,e^{-\lambda d}=-\Sigma\frac{2\mu_2}{\kappa_2+1}\left(\Delta\frac{\partial\tilde{v}}{\partial x}(\lambda,d)\right)_{b_x}^{\text{dislocation}}. \quad (56)$$

Similarly, dividing eqn (53) by μ_1 and subtracting from eqn (54) yields

$$-\frac{\kappa_1+1}{2\mu_1}C_2\,e^{-\lambda d}-\left(\frac{1}{\mu_2}-\frac{1}{\mu_1}\right)D_1\,e^{-\lambda d}-\left(\frac{1}{\mu_2}-\frac{1}{\mu_1}\right)\lambda d D_2\,e^{-\lambda d}+\frac{\kappa_2+1}{2\mu_2}D_2\,e^{-\lambda d}$$
$$-\left(\frac{1}{\mu_2}-\frac{1}{\mu_1}\right)D_3\,e^{\lambda d}-\left(\frac{1}{\mu_2}-\frac{1}{\mu_1}\right)\lambda d D_4\,e^{\lambda d}+\frac{\kappa_2+1}{2\mu_2}D_4\,e^{\lambda d}=-\frac{2\mu_2}{\kappa_2+1}\Sigma\left(\Delta\frac{\partial\tilde{u}}{\partial x}(\lambda,d)\right)_{b_x}^{\text{dislocation}}.$$

Using again the non-dimensional parameters α, β and Σ yields

$$-\left(\frac{\alpha-\beta}{1-\alpha}\right)D_1\,e^{-\lambda d}+\left[-\left(\frac{\alpha-\beta}{1-\alpha}\right)(1-\lambda d)+\frac{\Sigma}{2}\right]D_2\,e^{-\lambda d}-\left(\frac{\alpha-\beta}{1-\alpha}\right)D_3\,e^{\lambda d}$$
$$+\left[-\left(\frac{\alpha-\beta}{1-\alpha}\right)(1+\lambda d)+\frac{\Sigma}{2}\right]D_4\,e^{\lambda d}-\frac{1}{2}C_2\,e^{-\lambda d}=-\Sigma\frac{2\mu_2}{\kappa_2+1}\left(\Delta\frac{\partial\tilde{v}}{\partial x}(\lambda,d)\right)_{b_x}^{\text{dislocation}}. \quad (57)$$

The expressions for $(\Delta(\partial\tilde{u}/\partial x))_{b_x}^{\text{dislocation}}$ and $(\Delta(\partial\tilde{v}/\partial x))_{b_x}^{\text{dislocation}}$ are computed by taking the Fourier transform of eqns (32) and (35) and hence:

$$\left(\Delta\frac{\partial\tilde{u}}{\partial x}(\lambda,d)\right)_{b_x}^{\text{dislocation}}=\frac{1}{\pi}\left(\frac{\alpha(1-\lambda d)+\beta\lambda d}{(1+\alpha)}\right)e^{-\lambda d} \tag{58}$$

$$\left(\Delta\frac{\partial\tilde{v}}{\partial x}(\lambda,d)\right)_{b_x}^{\text{dislocation}}=\frac{1}{\pi}\left(\frac{\beta(1-\lambda d)+\alpha\lambda d)}{(1+\alpha)}\right)e^{-\lambda d}. \tag{59}$$

Interface Conditions at y = −c. At interface $y=-c$, the upper layer corresponds to material 2 and the lower layer to material 1. Substituting eqns (41) and (42) into eqn (50), and using coefficients D_1, D_2, D_3, D_4 above the interface and E_3, E_4 below the interface yields:

$$[(-D_1+D_2\lambda c)\,e^{\lambda c}+(-D_3+D_4\lambda c)\,e^{-\lambda c}]-(-E_3+E_4\lambda c)\,e^{-\lambda c}=0 \tag{60}$$

$$[-D_1+(1+\lambda c)D_2]\,e^{\lambda c}+[D_3+(1-\lambda c)D_4]\,e^{-\lambda c}-[E_3+(1-\lambda c)E_4]\,e^{-\lambda c}=0. \tag{61}$$

Substituting eqns (45) and (46) evaluated on both sides of the interface into eqn (51), yields:

$$\frac{1}{\mu_1}\left(E_3-E_4\lambda c+\frac{\kappa_1+1}{2}E_4\right)e^{-\lambda c}-\frac{1}{\mu_2}\left(D_1-D_2\lambda c-\frac{\kappa_2+1}{2}D_2\right)e^{\lambda c}$$
$$-\frac{1}{\mu_2}\left(D_3-D_4\lambda c+\frac{\kappa_2+1}{2}D_4\right)e^{-\lambda c}=-2\left(\Delta\frac{\partial\tilde{u}}{\partial x}(\lambda,-c)\right)_{b_x}^{\text{dislocation}}. \tag{62}$$

$$\frac{1}{\mu_1}\left(E_3+E_4-E_4\lambda c+\frac{\kappa_1+1}{2}E_4\right)e^{-\lambda c}-\frac{1}{\mu_2}\left(D_2-D_1+D_2\lambda c-\frac{\kappa_2+1}{2}D_2\right)e^{\lambda c}$$
$$-\frac{1}{\mu_2}\left(D_3+D_4-D_4\lambda c-\frac{\kappa_2+1}{2}D_4\right)e^{-\lambda c}=-2\left(\Delta\frac{\partial\tilde{v}}{\partial x}(\lambda,-c)\right)_{b_x}^{\text{dislocation}}. \tag{63}$$

Dividing eqn (61) by μ_2 and adding to eqn (63) gives:

$$\frac{\kappa_2+1}{2\mu_2}D_2\,e^{\lambda c}+\frac{\kappa_2+1}{2\mu_2}D_4\,e^{-\lambda c}+\left(\frac{1}{\mu_1}-\frac{1}{\mu_2}\right)E_3\,e^{-\lambda c}$$
$$+\left(\frac{-1+\lambda c}{\mu_2}+\frac{1-\lambda c}{\mu_1}-\frac{\kappa_1+1}{2\mu_1}\right)E_4\,e^{-\lambda c}=-2\left(\Delta\frac{\partial\tilde{v}}{\partial x}(\lambda,-c)\right)_{b_x}^{\text{dislocation}}.$$

Using the non-dimensional coefficients α, β and Σ of eqns (3) and (4) yields:

$$-\left(\frac{\alpha-\beta}{1-\alpha}\right)E_3\,e^{-\lambda c}+\left[-\left(\frac{\alpha-\beta}{1-\alpha}\right)(1-\lambda c)-\frac{1}{2}\right]E_4\,e^{-\lambda c}+\frac{\Sigma}{2}D_2\,e^{\lambda c}$$
$$+\frac{\Sigma}{2}D_4\,e^{-\lambda c}=-\Sigma\frac{2\mu_2}{\kappa_2+1}\left(\Delta\frac{\partial\tilde{v}}{\partial x}(\lambda,-c)\right)_{b_x}^{\text{dislocation}}. \tag{64}$$

Similarly, dividing eqn (61) by μ_2 and subtracting from eqn (62) gives:

$$\frac{\kappa_2+1}{2\mu_2}D_2\,e^{\lambda c}-\frac{\kappa_2+1}{2\mu_2}D_4\,e^{-\lambda c}+\left(\frac{1}{\mu_1}-\frac{1}{\mu_2}\right)E_3\,e^{-\lambda c}$$
$$+\left[-\lambda c\left(\frac{1}{\mu_1}-\frac{1}{\mu_2}\right)+\frac{\kappa_1+1}{2}\right]E_4\,e^{-\lambda c}=-2\left(\Delta\frac{\partial\tilde{u}}{\partial x}(\lambda,-c)\right)_{b_x}^{\text{dislocation}}.$$

Using the non-dimensional coefficients α, β and Σ of eqns (3) and (4) yields:

$$-\left(\frac{\alpha-\beta}{1-\alpha}\right)E_3\,e^{-\lambda c}+\left[\left(\frac{\alpha-\beta}{1-\alpha}\right)\lambda c+\frac{1}{2}\right]E_4\,e^{-\lambda c}+\frac{\Sigma}{2}D_2\,e^{\lambda c}$$
$$-\frac{\Sigma}{2}D_2\,e^{-\lambda c}=-\Sigma\frac{2\mu_2}{\kappa_2+1}\left(\Delta\frac{\partial\tilde{u}}{\partial x}(\lambda,-c)\right)_{b_x}^{\text{dislocation}}. \tag{65}$$

The expressions of $(\Delta(\partial\tilde{u}/\partial x))_{b_x}^{\text{dislocation}}$ and $(\Delta(\partial\tilde{v}/\partial x))_{b_x}^{\text{dislocation}}$ are computed by taking the Fourier transform of eqns (32) and (35) and hence:

$$\left(\Delta\frac{\partial\tilde{u}}{\partial x}(\lambda,-c)\right)_{b_x}^{\text{dislocation}}=-\frac{1}{\pi}\left(\frac{\alpha(1-\lambda c)+\beta\lambda c}{(1+\alpha)}\right)e^{-\lambda c} \tag{66}$$

$$\left(\Delta\frac{\partial\tilde{v}}{\partial x}(\lambda,-c)\right)_{b_x}^{\text{dislocation}}=\frac{1}{\pi}\left(\frac{\beta(1-\lambda c)+\alpha\lambda c}{(1+\alpha)}\right)e^{-\lambda c}. \tag{67}$$

Symbolic solution of the algebraic system of equations in the Fourier domain. Equations (52), (53), (56), (57), (60), (61), (64), and (65) can be put together in matrix form as

$$\begin{pmatrix}[M_1] & [M_2] & [0]\\ [M_3] & [0] & [M_4]\end{pmatrix}\begin{pmatrix}\{D\}\\ \{E\}\\ \{C\}\end{pmatrix}=\begin{pmatrix}\{v_1\}\\ \{v_2\}\end{pmatrix}, \tag{68}$$

where

$$[M_1]=e^{-\lambda d}\begin{bmatrix}-1 & \lambda c & -e^{-2\lambda c} & \lambda c\,e^{-2\lambda c}\\ -1 & (1+\lambda c) & e^{-2\lambda c} & (1-\lambda c)\,e^{-2\lambda c}\\ 0 & \frac{\Sigma}{2} & 0 & -\frac{\Sigma}{2}e^{-2\lambda c}\\ 0 & \frac{\Sigma}{2} & 0 & \frac{\Sigma}{2}e^{-2\lambda c}\end{bmatrix}, \tag{69}$$

$$[M_2]=e^{-\lambda(H+c)}\begin{bmatrix}1 & -\lambda c\\ -1 & \lambda c-1\\ -\frac{\alpha-\beta}{1-\alpha} & \frac{\alpha-\beta}{1-\alpha}\lambda c+\frac{1}{2}\\ -\frac{\alpha-\beta}{1-\alpha} & -\frac{\alpha-\beta}{1-\alpha}(1-\lambda c)-\frac{1}{2}\end{bmatrix},\quad [M_4]=e^{-\lambda(H+d)}\begin{bmatrix}1 & \lambda d\\ 1 & \lambda d-1\\ 0 & -\frac{1}{2}\\ 0 & -\frac{1}{2}\end{bmatrix}, \tag{70}$$

$$[M_3] = e^{-\lambda c}\begin{bmatrix} -e^{-2\lambda d} & -\lambda d e^{-2\lambda d} & -1 & -\lambda d \\ -e^{-2\lambda d} & (1-\lambda d)\,e^{-2\lambda d} & 1 & (1+\lambda d) \\ -\dfrac{\alpha-\beta}{1-\alpha}e^{-2\lambda d} & \left(-\dfrac{\alpha-\beta}{1-\alpha}\lambda d+\dfrac{\Sigma}{2}\right)e^{-2\lambda d} & -\dfrac{\alpha-\beta}{1-\alpha} & -\dfrac{\alpha-\beta}{1-\alpha}\lambda d-\dfrac{\Sigma}{2} \\ \dfrac{\alpha-\beta}{1-\alpha}e^{-2\lambda d} & \left(\dfrac{\alpha-\beta}{1-\alpha}(\lambda d-1)+\dfrac{\Sigma}{2}\right)e^{-2\lambda d} & -\dfrac{\alpha-\beta}{1-\alpha} & -\dfrac{\alpha-\beta}{1-\alpha}(\lambda d+1)+\dfrac{\Sigma}{2} \end{bmatrix}, \tag{71}$$

$$\{v_1\} = -\frac{2\mu_2\Sigma}{\kappa_2+1}e^{-\lambda(H+c)}\begin{Bmatrix} 0 \\ 0 \\ -\dfrac{1}{\pi}\left(\dfrac{\alpha(1-\lambda c)+\beta\lambda c}{(1+\alpha)}\right) \\ \dfrac{1}{\pi}\left(\dfrac{\beta(1-\lambda c)+\alpha\lambda c}{(1+\alpha)}\right) \end{Bmatrix}, \tag{72}$$

$$\{v_2\} = -\frac{2\mu_2\Sigma}{\kappa_2+1}e^{-\lambda(H+d)}\begin{Bmatrix} 0 \\ 0 \\ \dfrac{1}{\pi}\left(\dfrac{\alpha(1-\lambda d)+\beta\lambda d}{(1+\alpha)}\right) \\ \dfrac{1}{\pi}\left(\dfrac{\beta(1-\lambda d)+\alpha\lambda d}{(1+\alpha)}\right) \end{Bmatrix}. \tag{73}$$

The system (68) must be solved for the coefficients $D_1, \ldots, D_4$ contained in the vector $\{D\}$.

The matrices of eqn (68) are of size 4×4, 4×2, 4×4, and 4×2. This makes the system coupled and not readily solvable for $\{D\}$. Symbolic manipulation of system (68) can yield a symbolic solution (Graffeo, 1995). The matrices M_1, M_2, M_3 and M_4 were partitioned into smaller 2-row units, i.e.,

$$\begin{bmatrix} [M_{111}] & [M_{112}] & [M_{21}] & [0] \\ [M_{121}] & [M_{122}] & [M_{22}] & [0] \\ [M_{311}] & [M_{312}] & [0] & [M_{41}] \\ [M_{321}] & [M_{322}] & [0] & [M_{42}] \end{bmatrix}\begin{bmatrix} \{D_{12}\} \\ \{D_{34}\} \\ \{E\} \\ \{C\} \end{bmatrix} = \begin{bmatrix} \{v_{11}\} \\ \{v_{12}\} \\ \{v_{21}\} \\ \{v_{22}\} \end{bmatrix}. \tag{74}$$

Formal Gauss elimination was applied using the non-singular pivots M_{41} and M_{22}. The vectors $\{C\}$ and $\{E\}$ were eliminated, and hence

$$\begin{pmatrix} D_1 \\ D_2 \end{pmatrix} = \{D_{12}\} = [M^*_{21}] - ([M^*_{22}][M^*_{12}]^{-1}[M^*_{11}])^{-1}([v^*_{22}] - [M^*_{22}][M^*_{12}]^{-1}[v^*_{11}]), \tag{75}$$

$$\begin{pmatrix} D_3 \\ D_4 \end{pmatrix} = \{D_{34}\} = [M^*_{12}] - ([M^*_{11}][M^*_{12}]^{-1}[M^*_{22}])^{-1}([v^*_{11}] - [M^*_{11}][M^*_{21}]^{-1}[v^*_{22}]), \tag{76}$$

where

$$[M_{11}^{*}] = [M_{321}] - [M_{42}][M_{41}]^{-1}[M_{311}], \quad [M_{21}^{*}] = [M_{121}] - [M_{22}][M_{21}]^{-1}[M_{111}], \tag{77}$$

$$[M_{12}^{*}] = [M_{322}] - [M_{42}][M_{41}]^{-1}[M_{312}], \quad [M_{22}^{*}] = [M_{122}] - [M_{22}][M_{21}]^{-1}[M_{112}], \tag{78}$$

$$[v_{11}^{*}] = [v_{22}] - [M_{42}][M_{41}]^{-1}[v_{21}], \quad [v_{22}^{*}] = [v_{12}] - [M_{22}][M_{21}]^{-1}[v_{11}]. \tag{79}$$

Evaluation of the coefficients $D_1, \ldots, D_4$ was done at λ-values in the range $(0, \lambda_{max})$, where λ_{max} is the upper limit of the truncated Fourier domain.

Correction stress field for b_y

In this case $b_x = 0$, and $b_y = 1$, and the equations of the problem are the same as in the Case b_x, except that U is odd with respect to x and X is even with respect to x. Hence, we apply the Fourier sine transform to U and the Fourier cosine transform to X. Denoting

$$\mathcal{F}_s(U) = \tilde{U} = \frac{2}{\pi}\int_0^\infty U \sin \lambda x \, dx, \quad \mathcal{F}_c(X) = \tilde{X} = \frac{2}{\pi}\int_0^\infty X \cos \lambda x \, dx, \tag{80}$$

and following the same steps as in Case b_x, we obtain the following integral representations

$$U(x,y) = b_y \int_0^\infty \left[\left(\frac{B_1}{\lambda^2} + \frac{B_2}{\lambda} y\right)e^{-\lambda y} + \left(\frac{B_3}{\lambda^2} + \frac{B_4}{\lambda} y\right)e^{\lambda y}\right] \sin \lambda x \, d\lambda,$$

$$X(x,y) = -b_y \int_0^\infty \frac{1}{2\lambda^2}[B_2 e^{-\lambda y} + B_4 e^{\lambda y}) \cos \lambda x \, d\lambda. \tag{81}$$

The minus sign in the X representation appears when using eqn (6). The coefficients B_i are denoted: F_i in layer 1, G_i in layer 2 and H_i in layer 3. From the far-field conditions it follows that $F_3 = F_4 = H_1 = H_2 = 0$. The interface conditions are introduced in the same manner as in the Case b_x, and finally we get

$$\begin{pmatrix} [M_1] & [M_2] & 0 \\ [M_3] & 0 & [M_4] \end{pmatrix} \begin{Bmatrix} \{G\} \\ \{H\} \\ \{F\} \end{Bmatrix} = \begin{pmatrix} \{w_1\} \\ \{w_2\} \end{pmatrix}, \tag{82}$$

where the matrices $[M_1]$–$[M_4]$ are given by eqns (69)–(71) and $\{w_i\}$ have the expressions

$$\{w_1\} = -\frac{2\mu_2 \Sigma}{\kappa_2 + 1} e^{-\lambda(H+c)} \begin{Bmatrix} 0 \\ 0 \\ \frac{1}{\pi}\left(\frac{-\beta(1+\lambda c) + \alpha\lambda c}{(1+\alpha)}\right) \\ \frac{1}{\pi}\left(\frac{-\alpha(1+\lambda c) + \beta\lambda c}{(1+\alpha)}\right) \end{Bmatrix},$$

$$\{w_2\} = -\frac{2\mu_2 \Sigma}{\kappa_2 + 1} e^{-\lambda(H+d)} \begin{Bmatrix} 0 \\ 0 \\ \frac{1}{\pi}\left(\frac{-\beta(1+\lambda d) + \alpha\lambda d}{(1+\alpha)}\right) \\ \frac{1}{\pi}\left(\frac{\alpha(1+\lambda d) - \beta\lambda d}{(1+\alpha)}\right) \end{Bmatrix}. \tag{83}$$

After formal elimination of $\{H\}$ and $\{F\}$, we get

$$\begin{pmatrix} G_1 \\ G_2 \end{pmatrix} = \{G_{12}\} = [M_{21}^*] - ([M_{22}^*][M_{12}^*]^{-1}[M_{11}^*])^{-1}([w_{22}^*] - [M_{22}^*][M_{12}^*]^{-1}[w_{11}^*]), \quad (84)$$

$$\begin{pmatrix} G_3 \\ G_4 \end{pmatrix} = \{G_{34}\} = [M_{12}^*] - ([M_{11}^*][M_{21}^*]^{-1}[M_{22}^*])^{-1}([w_{11}^*] - [M_{11}^*][M_{21}^*]^{-1}[w_{22}^*]), \quad (85)$$

where the matrices of the right hand side are given in eqns (77)–(79).

Superposition of problem 1 *and problem* 2

The full stress field in any point of the plane is obtained superposing the effects. Generally we may write

$$\begin{aligned} \sigma &= \sigma^{\text{Problem 1}} + \sigma^{\text{Problem 2}} \\ &= \sigma^{\text{dislocation}} + \sigma^{\text{correction}} \end{aligned} \quad (86)$$

where $\sigma^{\text{dislocation}}$ represents the state of stress given in Problem 1 by eqn (29). The correction stresses $\sigma^{\text{correction}}$, are calculated in Problem 2 with eqns (75) and (76). For $b_x = 1$, use the coefficients $D_1, \ldots, D_4$ given by eqns (75) and (76) to get:

$$\begin{aligned} (\sigma_{xx})_{b_x}^{\text{correction}} &= \int_0^\infty \{[D_1 + (\lambda y - 2)D_2]\, e^{-\lambda y} + [D_3 + (\lambda y + 2)D_4]\, e^{\lambda y}\} \cos \lambda x \, \mathrm{d}\lambda, \\ (\sigma_{yy})_{b_x}^{\text{correction}} &= -\int_0^\infty [(D_1 + D_2 \lambda y)\, e^{-\lambda y} + (D_3 + D_4 \lambda y)\, e^{\lambda y}] \cos \lambda x \, \mathrm{d}\lambda, \\ (\sigma_{xy})_{b_x}^{\text{correction}} &= \int_0^\infty \{[D_1 + (\lambda y - 1)D_2]\, e^{-\lambda y} + [D_3 + (\lambda y + 1)D_4]\, e^{\lambda y}\} \sin \lambda x \, \mathrm{d}\lambda. \end{aligned} \quad (87)$$

For $b_y = 1$, use the coefficients $G_1, \ldots, G_4$ given by eqns (84) and (85) to get

$$\begin{aligned} (\sigma_{xx})_{b_y}^{\text{correction}} &= \int_0^\infty \{[G_1 + (\lambda y - 2)G_2]\, e^{-\lambda y} + [G_3 + (\lambda y + 2)G_4]\, e^{\lambda y}\} \sin \lambda x \, \mathrm{d}\lambda, \\ (\sigma_{yy})_{b_y}^{\text{correction}} &= -\int_0^\infty [(G_1 + G_2 \lambda y)\, e^{-\lambda y} + (G_3 + G_4 \lambda y)\, e^{\lambda y}] \sin \lambda x \, \mathrm{d}\lambda, \\ (\sigma_{xy})_{b_y}^{\text{correction}} &= \int_0^\infty \{[G_1 + (\lambda y - 1)G_2]\, e^{-\lambda y} + [G_3 + (\lambda y + 1)G_4]\, e^{\lambda y}\} \cos \lambda x \, \mathrm{d}\lambda. \end{aligned} \quad (88)$$

Hence, at $y = 0$, at the crack line, the stress field induced by the dislocation is given by

$$\sigma_{xx}(x, 0) = \frac{\mu_2}{4\pi(1 - \nu_2)} \left(\frac{2b_y}{x} + g_x(x) b_x + g_y(x) b_y \right), \quad (89)$$

$$\sigma_{xy}(x, 0) = \frac{\mu_2}{4\pi(1 - \nu_2)} \left(\frac{2b_x}{x} + f_{xx}(x) b_x + f_{xy}(x) b_y \right), \quad (90)$$

$$\sigma_{yy}(x, 0) = \frac{\mu_2}{4\pi(1 - \nu_2)} \left(\frac{2b_y}{x} + f_{yx}(x) b_x + f_{yy}(x) b_y \right). \quad (91)$$

The correction functions $g_i(x)$ and $f_{ij}(x)$, $i,j = 1, 2$, used in eqns (89)–(91), are derived from eqns (87) and (88) by taking $y = 0$ and dividing by $\mu_2/4\pi(1-\nu_2)$, i.e.,

$$g_x(x) = \frac{4\pi(1-\nu_2)}{\mu_2}\int_0^\infty [D_1(\lambda)+2D_2(\lambda)+D_3(\lambda)+2D_4(\lambda)]\sin\lambda x\,\mathrm{d}\lambda,$$

$$g_y(x) = \frac{4\pi(1-\nu_2)}{\mu_2}\int_0^\infty [G_1(\lambda)+2G_2(\lambda)+G_3(\lambda)+2G_4(\lambda)]\cos\lambda x\,\mathrm{d}\lambda, \tag{92}$$

or

$$f_{xx}(x) = \frac{4\pi(1-\nu_2)}{\mu_2}\int_0^\infty [-D_1(\lambda)+D_2(\lambda)+D_3(\lambda)+D_4(\lambda)]\sin\lambda x\,\mathrm{d}\lambda,$$

$$f_{xy}(x) = \frac{4\pi(1-\nu_2)}{\mu_2}\int_0^\infty [G_1(\lambda)-G_2(\lambda)-G_3(\lambda)-G_4(\lambda)]\cos\lambda x\,\mathrm{d}\lambda,$$

$$f_{yx}(x) = \frac{4\pi(1-\nu_2)}{\mu_2}\int_0^\infty [-D_1(\lambda)-D_3(\lambda)]\cos\lambda x\,\mathrm{d}\lambda,$$

$$f_{yy}(x) = \frac{4\pi(1-\nu_2)}{\mu_2}\int_0^\infty [-G_1(\lambda)-G_3(\lambda)]\cos\lambda x\,\mathrm{d}\lambda. \tag{93}$$

The Fourier transforms contained in eqns (92) and (93) were performed numerically using an adaptation of the Fast Fourier Transform (FFT) method.

THE INTEGRAL EQUATION AND ITS SOLUTION

Setup of the integral equation

Consider Fig. 2, with the crack in the adhesive layer extending along the negative x-axis from 0^- to $-\infty$. The crack is modeled by an unknown distribution of dislocations to be determined from the boundary conditions and the load-like far-field quantities, K_I^∞, K_{II}^∞, and T^∞. The following matrix notations are used:

$$\mathbf{b}(x) = \begin{Bmatrix} b_x(x) \\ b_y(x) \end{Bmatrix}, \quad \mathbf{f}(x) = \begin{bmatrix} f_{xx}(x) & f_{xy}(x) \\ f_{yx}(x) & f_{yy}(x) \end{bmatrix}, \quad \mathbf{p}(x) = \begin{Bmatrix} p_x(x,0) \\ p_y(x,0) \end{Bmatrix},$$

$$\mathbf{u}(x) = \begin{Bmatrix} u(x) \\ v(x) \end{Bmatrix}, \quad \mathbf{K} = \begin{Bmatrix} K_{II} \\ K_I \end{Bmatrix} \tag{94}$$

where the functions $f_{xx}(x)$, $f_{xy}(x)$, and $f_{yy}(x)$ are given eqn (93). The traction-free condition on the crack faces ($y = 0$) is written as

$$\mathbf{p}(x) = \frac{\mu_2}{4\pi(1-\nu_2)}\int_{-\infty}^0 \left[\frac{2\mathbf{b}(\xi)}{x-\xi}+\mathbf{f}(x-\xi)\mathbf{b}(\xi)\right]\mathrm{d}\xi = 0. \tag{95}$$

By definition, the relation between crack face displacements and the distribution of dislocations is

$$\mathbf{u}(x)^+ - \mathbf{u}(x)^- = \int_x^0 \mathbf{b}(\xi)\,\mathrm{d}\xi \;\Rightarrow\; \frac{\partial}{\partial x}(\mathbf{u}(x)^+ - \mathbf{u}(x)^-) = -\mathbf{b}(x)\,\mathrm{d}x. \tag{96}$$

Recall Williams' (1952) relation:

$$\mathbf{u}(x)^+ - \mathbf{u}(x)^- = \frac{\mathbf{K}}{\mu}\sqrt{\frac{x}{2\pi}}(\kappa+1). \tag{97}$$

Differentiating eqn (97) and substituting in eqn (96) yields

$$\mathbf{b}(x) \sim \frac{\kappa_2+1}{2\mu_2}\frac{\mathbf{K}}{\sqrt{-2\pi x}}. \tag{98}$$

Applying eqn (98) in the adhesive (material 2) i.e. very close to the crack tip, we write:

$$\mathbf{b}(\xi) \sim \frac{\kappa+1}{2\mu}\frac{\mathbf{K}}{\sqrt{-2\pi\xi}} \quad \text{when } \xi \to 0^-, \tag{99}$$

whereas in the adherent (material 1) we get:

$$\mathbf{b}(\xi) \sim \frac{\kappa_1+1}{2\mu_1}\frac{\mathbf{K}^\infty}{\sqrt{-2\pi\xi}} \quad \text{when } \xi \to -\infty. \tag{100}$$

The integral eqn (95) and the additional condition (100) must be solved to determine the unknown distribution of dislocations, $\mathbf{b}(x)$. Equation (99) can be then used to determine the near-field stress intensity factors in the adhesive.

The infinite interval $(-\infty, 0)$ can be conveniently changed to the finite interval $(-1, 1)$ through the change of variables

$$x = \frac{u-1}{u+1}, \quad \xi = \frac{t-1}{t+1}, \quad u, t \in (-1, 1) \tag{101}$$

and denoting $\mathbf{c}(t) = \mathbf{b}(\xi(t))$, eqn (95) becomes:

$$\int_{-1}^{1} \frac{u+1}{(u-t)(t+1)}\mathbf{c}(t)\,\mathrm{d}t + \int_{-1}^{1} \mathbf{F}(x(u)-\xi(t))\mathbf{c}(t)\frac{\mathrm{d}t}{(t+1)^2} = 0, \tag{102}$$

while eqns (99) and (100) take the form

$$\mathbf{c}(t) \to \frac{2}{\sqrt{2\pi}}\sqrt{\frac{1+t}{1-t}}\left(\frac{\kappa_2+1}{2\mu_2}\right)\mathbf{K} \quad \text{for } t \to 1^-, \tag{103a}$$

$$\mathbf{c}(t) \to \frac{2}{\sqrt{2\pi}}\sqrt{\frac{1+t}{1-t}}\left(\frac{\kappa_1+1}{2\mu_1}\right)\mathbf{K}^\infty \quad \text{for } t \to -1^+. \tag{103b}$$

Chebyshev series expansion

The solution is sought in terms of a truncated Chebyshev series:

$$\mathbf{c}(t) \approx \sqrt{\frac{1+t}{1-t}} \cdot \sum_{k=0}^{N} T_k(t)\mathbf{a}_k, \tag{104}$$

where N is the number of terms, $T_k(t)$ are Chebyshev polynomials of the first kind and order k, i.e.,

$$T_k(t) = \cos(k \arccos(t)) \quad \text{and} \quad \mathbf{a}_k = \begin{Bmatrix} a_{1,k} \\ a_{2,k} \end{Bmatrix} = \begin{Bmatrix} a_1 \\ a_2 \end{Bmatrix}_k. \tag{105}$$

The $2(N+1)$ coefficients, $\mathbf{a}_k$, in the Chebyshev series expansion have to be determined numerically. Taking the limit $t \to 1^-$ and $t \to -1^+$ in eqns (102) and (103), respectively, yields the direct relation between the near-field and far-field stress intensity factors and Chebyshev coefficients:

$$\mathbf{K} = \sqrt{\frac{\pi}{2}} \frac{2\mu_2}{\kappa_2 + 1} \sum_{k=0}^{\infty} \mathbf{a}_k \tag{106}$$

$$\sum_{k=0}^{\infty} (-1)^k \mathbf{a}_k = \sqrt{\frac{2}{\pi}} \left(\frac{\kappa_2 + 1}{2\mu_2} \right) \frac{1-\alpha}{1+\alpha} \mathbf{K}^{\infty}. \tag{107}$$

Substitution of eqn (104) into eqn (101) yields the discretized form of the integral equation:

$$-\pi(1+u) \sum_{k=1}^{\infty} U_{k-1}(u)\mathbf{a}_k + \sum_{k=0}^{\infty} \mathbf{D}_k(u)\mathbf{a}_k = 0, \tag{108}$$

where

$$U_k(u) = \frac{\sin(k \arccos u)}{\sqrt{1-u^2}} \quad \text{and} \quad \mathbf{D}_k(u) = \int_{-1}^{1} \frac{\mathbf{f}(x(u) - \xi(t))}{1+t} \frac{T_k(t)}{\sqrt{1-t^2}} \mathrm{d}t. \tag{109}$$

Collocation of the discretized integral equation

The discretized integral eqn (108) is transformed into a system of $N \times N$ equations by evaluation at N Gauss–Legendre collocation points:

$$-\pi(1+u_i) \sum_{k=1}^{N} U_{k-1}(u_i)\mathbf{a}_k + \sum_{k=0}^{N} \mathbf{D}_k(u_i)\mathbf{a}_k = 0 \quad i = 0, \ldots, N \quad u_i \in (-1, 1). \tag{110}$$

Adding eqn (107) yields, in matrix notations,

$$\begin{bmatrix} \mathbf{D}_{0,0} & -\pi(1+u_0)U_0\mathbf{I} + \mathbf{D}_{0,1} & \cdots & -\pi(1+u_0)U_{N-1}\mathbf{I} + \mathbf{D}_{0,N} \\ \mathbf{D}_{1,0} & -\pi(1+u_1)U_0\mathbf{I} + \mathbf{D}_{1,1} & \cdots & -\pi(1+u_1)U_{N-1}\mathbf{I} + \mathbf{D}_{1,N} \\ \vdots & \vdots & \vdots & \vdots \\ \mathbf{D}_{n,0} & -\pi(1+u_N)U_0\mathbf{I} + \mathbf{D}_{n,1} & \cdots & -\pi(1+u_N)U_{N-1}\mathbf{I} + \mathbf{D}_{N,N} \\ I & -\mathbf{I} & \cdots & (-1)^N\mathbf{I} \end{bmatrix} \begin{Bmatrix} \mathbf{a}_0 \\ \mathbf{a}_1 \\ \vdots \\ \mathbf{a}_{N-1} \\ \mathbf{a}_N \end{Bmatrix} = \begin{Bmatrix} 0 \\ 0 \\ \vdots \\ 0 \\ \mathbf{v} \end{Bmatrix} \tag{111}$$

where $\mathbf{I}$ is the 2×2 identity matrix, $\mathbf{v}$ is the "data", i.e.,

$$\mathbf{v} = \sqrt{\frac{2}{\pi}} \left(\frac{\kappa_2 + 1}{2\mu_2} \right) \frac{1-\alpha}{1+\alpha} \mathbf{K}^{\infty}, \tag{112}$$

and $\mathbf{D}_{i,k}$ are the matrix coefficients,

$$\mathbf{D}_{i,k} = \int_{-1}^{1} \frac{\mathbf{f}(x(u_i)-\xi(t))}{1+t} \frac{T_k(t)}{\sqrt{1-t^2}} \mathrm{d}t. \tag{113}$$

Evaluation of the singular integrals defining the matrix coefficients $\mathrm{D_{i,k}}$

Evaluation of the matrix coefficients $\mathbf{D}_{i,k}$ involves certain singular integrals that need to be treated with special attention. Writing eqn (109) for $k+1$

$$\mathbf{D}_{k+1}(u) = \int_{-1}^{1} \frac{\mathbf{f}(x(u)-\xi(t))}{1+t} \frac{T_{k+1}(t)}{1-t^2} \mathrm{d}t, \tag{114}$$

and using the recurrence relation between Chebyshev polynomials

$$T_{k+1}(t) = 2tT_k(t) - T_{k-1}(t), \quad T_0 = 1, \quad T_1 = t, \tag{115}$$

yields

$$\mathbf{D}_{k+1}(u) = 2\mathbf{E}_k(u) - 2\mathbf{D}_k(u) - \mathbf{D}_{k-1}(u), \quad k > 1, \quad \text{and} \quad \mathbf{D}_1(u) = \mathbf{E}_0(u) - \mathbf{D}_0(u), \tag{116}$$

where

$$\mathbf{E}_k(u) = \int_{-1}^{1} \mathbf{f}(x(u)-\xi(t)) \frac{T_k(t)}{\sqrt{1-t^2}} \mathrm{d}t, \quad k \geqslant 0 \quad \text{and} \quad \mathbf{D}_0(u) = \int_{-1}^{1} \frac{\mathbf{f}(x(u)-\xi(t))}{1+t} \frac{1}{1-t^2} \mathrm{d}t. \tag{117}$$

Thus, the evaluation of eqn (109) has been reduced to the evaluation of only two integrals, $\mathbf{E}_k(u)$ and $\mathbf{D}_0(u)$. The integral $\mathbf{E}_k(u)$ can be computed directly using Gauss–Chebyshev quadrature

$$\mathbf{E}_k(u) \approx \frac{\pi}{n} \sum_{j=0}^{n} \mathbf{f}(x(u)-\xi(t_j)) T_k(t_j) \quad \text{where } t_j = \cos\left(\frac{2_j+1}{2n}\right), \quad n = 40. \tag{118}$$

The integral $\mathbf{D}_0(u)$ requires further attention, since it has a singular point at $t \to -1$ due to the presence of $t+1$ in the denominator. Making the change in variable $t = (1-\eta)/(1+\eta)$, we obtain

$$\mathbf{D}_0(u) = \frac{1}{2} \int_0^{\infty} \frac{\mathbf{f}(x(u)+\eta)}{\sqrt{\eta}} \mathrm{d}\eta. \tag{119}$$

The integral (119) has an integratable singularity at $\eta = 0$. Two methods were used in parallel to compute the integral (119): the Singularity Removal Method and the Finite-Part Regularization Technique. These methods are described next.

Singularity removal method

Using the change of variable $\eta \to \rho^2$, expression (119) becomes

$$\mathbf{D}_0(u) \int_0^\infty \mathbf{f}(x(u)+\rho^2)\,\mathrm{d}\eta = \int_0^{\rho_0} \mathbf{f}(x(u)+\rho^2)\,\mathrm{d}\eta + \int_{\rho_0}^\infty \mathbf{f}(x(u)+\rho^2)\,\mathrm{d}\eta$$

$$\text{where } \rho_0 = \sqrt{\frac{1-u}{1+u}}. \tag{120}$$

Finite-part regularization technique

Integral (119) can be written as

$$\mathbf{D}_0(u) = \lim_{\varepsilon \to 0} \frac{\sqrt{\pi}}{2} \int_0^\infty \frac{\mathbf{f}(x(u)+\eta)}{\sqrt{\pi\eta}}\,\mathrm{d}\eta. \tag{121}$$

Denoting

$$\mathbf{f}^s(x) = \begin{bmatrix} 0 & f_{xy}(x) \\ f_{yx}(x) & 0 \end{bmatrix} \quad \text{and} \quad f^a(x) = \begin{bmatrix} f_{xx}(x) & 0 \\ 0 & f_{yy}(x) \end{bmatrix} \tag{122}$$

the symmetric and antisymmetric part of $F(x)$ integral, one can write eqn (121) as

$$\mathbf{D}_0(u) = \frac{\sqrt{\eta}}{2} Pf\left(\frac{1}{\sqrt{\pi x}}\right)_{x>0} * (\mathbf{f}^s(x) - \mathbf{f}^a(x)), \quad x = \frac{1-u}{1+u} \tag{123}$$

where the symbol $*$ signifies the convolution integral, e.g., $f * g = \int f(\xi) g(x-\xi)\,\mathrm{d}\xi$, while

$$\frac{1}{\sqrt{\pi}} Pf\left(\frac{1}{\sqrt{x}}\right)_{x>0} \tag{124}$$

is the Finite Part distribution of $1/\sqrt{\pi x}$ (Zemanian, 1965; Ionita, 1993). We use a regularization of expression (124) through the following Dirac delta distribution sequence (Kecs and Teodorescu, 1974):

$$\delta_{\varepsilon_n}(x) = \frac{1}{\pi} \frac{\varepsilon_n}{x^2 + \varepsilon_n^2}, \quad \text{where } \lim_{n\to\infty} \varepsilon_n = 0, \quad \text{and} \quad \lim_{\varepsilon_n \to 0} \delta_{\varepsilon_n}(x) = \delta(x) \tag{125}$$

where $\delta(x)$ is Dirac delta distribution. Hence,

$$\varphi_{\varepsilon_n}(x) = \frac{1}{\pi} Pf\left(\frac{1}{\sqrt{x}}\right)_{x>0} * \delta_{\varepsilon_n}(x) = \frac{\cos\left(\frac{\theta_{\varepsilon_n}}{2}\right)}{\sqrt{\pi r_{\varepsilon_n}}}, \quad \theta_{\varepsilon_n} = \arctan\frac{\varepsilon_n}{x}, \quad r_{\varepsilon_n} = \sqrt{x^2+\varepsilon_n^2}. \tag{126}$$

The limit $\varepsilon_n \to 0$ of eqn (126) yields expression (124), i.e.,

$$\lim_{\varepsilon_n \to 0} \varphi_n(x) = Pf\left(\frac{1}{\sqrt{\pi x}}\right)_{x>0}.$$

Using (126) in relation (123) gives the following evaluation of the $\mathbf{D}_0(u)$ integral:

$$\mathbf{D}_0(u) = \frac{\sqrt{\pi}}{2} \lim_{\varepsilon_n \to 0} \varphi_{\varepsilon_n}(x) * (\mathbf{f}^c(x) - \mathbf{f}^a(x)), \quad x = \frac{1-u}{1+u}. \tag{127}$$

After the matrix coefficients $\mathbf{D}_{i,k}$ are evaluated, the linear algebraic system (111) is solved through standard numerical routines, and the solution represents the Chebyshev coefficients, contained in the vector matrix $\mathbf{a}_k$, $k = 0, \ldots, N$. Substitution of these coefficients into the series expansion (104) yields the dislocations distribution, and thus the problem is solved.

EVALUATION OF THE NEAR-FIELD STRESS INTENSITY FACTORS, K_I AND K_{II}

The Chebyshev coefficients, contained in the vector matrix $\mathbf{a}_k$, $k = 0, \ldots, N$ can be used to calculate the near-field stress intensity factors, K_I and K_{II} in the adhesive layer. Recall eqn (106),

$$\mathbf{K} = \sqrt{\frac{\pi}{2}} \frac{2\mu_2}{\kappa_2 + 1} \sum_{k=0}^{\infty} \mathbf{a}_k, \quad \text{where } \mathbf{K} = \begin{Bmatrix} K_{II} \\ K_I \end{Bmatrix}. \tag{128}$$

Hence, the near-field stress intensity factors are calculated as

$$K_I = \sqrt{\frac{\pi}{2}} \frac{2\mu_2}{\kappa_2 + 1} \sum_{k=0}^{\infty} a_{k,2} \quad \text{and} \quad K_{II} = \sqrt{\frac{\pi}{2}} \frac{2\mu_2}{\kappa_2 + 1} \sum_{k=0}^{\infty} a_{k,1}. \tag{129}$$

EVALUATION OF THE COEFFICIENTS c_I AND c_{II} OF THE T-STRESS

The stress σ_{xx} at any point on the x-axis is calculated with the integral:

$$\sigma_{xx}(x) = \frac{\mu_2}{4\pi(1-\nu_2)} \int_{-\infty}^{0} \left[\frac{2b_x \xi}{x-\xi} \mathrm{d}\xi + \int_{-\infty}^{0} \mathbf{g}(x-\xi) \cdot \mathbf{b}(\xi) \, \mathrm{d}\xi \right] \tag{130}$$

where the row matrix $\mathbf{g}(x) = [g_x(x) \quad g_y(x)]$ contains the expressions given by eqn (92). Substituting the Chebyshev series expansion (104) into eqn (130) yields

$$\sigma_{xx}(x(u)) = \frac{\mu_2}{4\pi(1-\nu_2)} \left[-2\pi(1+u) \sum_{k=1}^{\infty} U_{k-1}(u) a_{2,k} + \sum_{k=0}^{\infty} \mathbf{H}_k(u) \mathbf{a}_k \right] \tag{131}$$

where

$$\mathbf{H}_k(u) = \int_{-1}^{1} \frac{\mathbf{g}(x(u) - \xi(t))}{1+t} \frac{T_k(t)}{\sqrt{1-t^2}} \mathrm{d}t. \tag{132}$$

The T-stress in the adhesive layer is estimated by evaluating σ_{xx} on the crack faces very close behind crack tip, i.e.,

$$T = \lim_{x \to 0^-} \sigma_{xx}(x) = \lim_{u \to 1^-} \sigma_{xx}(x(u)). \tag{133}$$

Substituting eqn (131) into eqn (133) yields

$$T = \frac{\mu_2}{4\pi(1-\nu_2)}\left[-4\pi\sum_{k=1}^{\infty} k a_{2,k} + \sum_{k=0}^{\infty} \mathbf{H}_k(1)\mathbf{a}_k\right]. \tag{134}$$

The evaluation of $\mathbf{H}_k(1)$ was done without numerical difficulties using the Gauss–Chebyshev quadrature:

$$\mathbf{H}_k(1) = \frac{\pi}{n}\sum_{j=1}^{n} \frac{\mathbf{g}(-\xi(t_j))}{1+t_j} T_k(t_j), \quad t_j = \cos\left(\frac{2j-1}{2n}\pi\right). \tag{135}$$

Linear dependence is assumed between the local T-stress and the far field stress intensity factors, K_I^{∞} and K_{II}^{∞}, i.e, $T = c_I K_I^{\infty} + c_{II} K_{II}^{\infty}$. Hence, c_I and c_{II} are calculated by solving the problem for $K_I = 1$, $K_{II} = 0$, and for $K_I = 0$, $K_{II} = 1$, respectively.

CONVERGENCE STUDIES AND NUMERICAL RESULTS

Numerical cases were studied to assess the convergence properties of the method and to obtain numerical values for the c_I and c_{II} coefficients of the local T-stress. In one study, realistic values of the material parameters were used, and the Aluminum/Epoxy adherend/adhesive pair was chosen with $\mu_1 = 26.3$, $\nu_1 = 0.35$, $\mu_2 = 1.5$, $\nu_2 = 0.34$, $\alpha = 0.8936$, $\beta = 0.2431$. Two other cases were run with round values of the Dundurs parameters ($\alpha = 0.8$, $\beta = 0.3$, and $\alpha = 0.9$, $\beta = 0.2$) in order to facilitate direct comparison with the results published by Fleck *et al.* (1991). In all cases, the crack-positioning parameter was taken as $c/H = 0.6$. Several convergence studies were performed. In these studies we solved the problem for an increasing numerical size ($N = 10$, 20, 30, and 40), and examined the behavior of the Chebyshev coefficients, of the stress intensity factors error parameter, and of the c_I and c_{II} coefficients.

Convergence of the Chebyshev coefficients

Figure 7 shows the variation of the $a_{1,k}$, $a_{2,k}$ Chebyshev series coefficients with k for $N = 20$, under two loading conditions, mode I loading ($K_I = 1, K_{II} = 0$), and mode II loading ($K_I = 0, K_{II} = 1$). Recall that, in a homogeneous material, mode I loading induces only $a_{2,k}$ coefficients, while mode II loading induces only $a_{1,k}$. In our case of mixed materials, mode I loading will induce both $a_{2,k}$ and $a_{1,k}$ coefficients, but the former will be dominant, while the latter will be much smaller and will serve as corrections. For mode II, the same situation occurs, but with the subscripts reversed, i.e., $a_{1,k}$ are dominant and $a_{2,k}$ are corrections. The correction Chebyshev series coefficients can be also viewed as coupling terms generating mode II stress intensity factors under mode I loading and vice-versa. The coupling Chebyshev series coefficients were found to be two orders of magnitudes lower than the dominant Chebyshev series coefficients.

Note that Fig. 7 presents separately the dominant Chebyshev series coefficients and the correction Chebyshev series coefficients. Though the absolute value of the correction Chebyshev series coefficients is small compared to the dominant Chebyshev series coefficients, their contribution is paramount in revealing the differences between the classical homogeneous case and the bi-material case studied here. Examination of Fig. 7 indicates that, for this value of N, the dominant coefficient converge rapidly towards zero (Fig. 7(a)), while the correction coefficients converge much slower (Fig. 7(b)). A better convergence was notices for $N = 40$. However, for $N = 30$, a case of bad convergence (or even non-convergence) was sighted. Figure 8 presents the Chebyshev series coefficients for mode I and $N = 30$. In Fig. 8(a) we see that the dominant Chebyshev series coefficients converge very slowly and present a "beats" phenomenon. In Fig. 8(b) we observe that the correction Chebyshev series coefficients do not seem to converge at all and maintain large amplitudes even at $k = N$.

Similar patterns of behavior were obtained for the other combinations of α and β parameters. These numerical experiments indicated that the case $N = 30$ had numerical

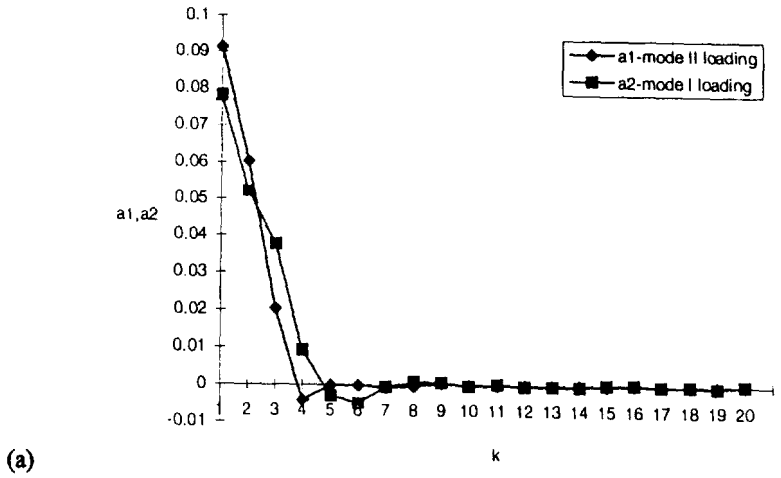

(a)

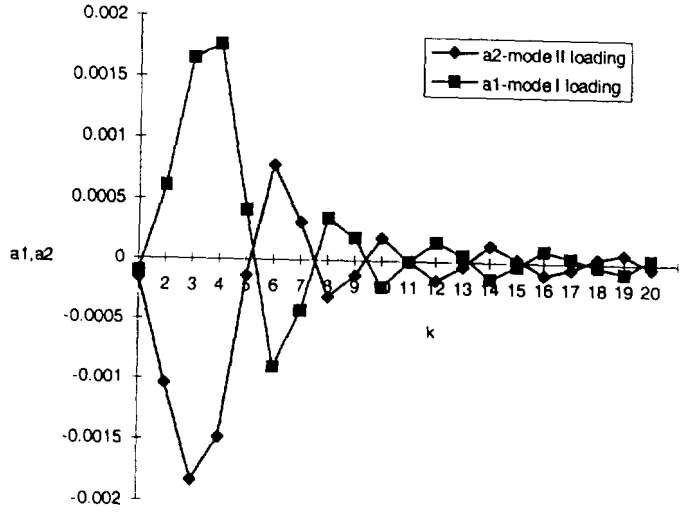

b)

Fig. 7. Chebyshev series coefficients, $a_{1,k}$, $a_{2,k}$, for $N = 20$ and $\alpha = 0.8$, $\beta = 0.3$: (a) strong convergence of the dominant Chebyshev series coefficients; (b) weaker convergence of the correction Chebyshev series coefficients.

problems and did not converge properly, while the cases $N = 20$ and $N = 40$ did not have numerical problems and convergence satisfactorily.

Convergence of the reconstructed dislocations distribution

The Chebyshev series coefficients can be used to reconstruct the dislocation distribution using eqn (47). Note that this equation contains a singular part $(1+t)^{1/2}(1-t)^{1/2}$, multiplying the Chebyshev series. In our studies, we concentrated our attention on the Chebyshev series and used the expression

$$\begin{Bmatrix} c_1^*(t) \\ c_2^*(t) \end{Bmatrix} = \sum_{k=0}^{N} T_k(t) \begin{Bmatrix} a_{1,k} \\ a_{2,k} \end{Bmatrix}. \tag{136}$$

Figure 9 presents plots of eqn (136) for $N = 10$, 20, 30 and 40 where Fig. 9(a) presents the dominant part of the dislocations distribution, i.e. $c_2^*(t)$ for mode I loading and $\alpha = 0.8$, $\beta = 0.3$. Note that the reconstructed curves for $N = 10$, 20 and 30 are almost indistinguishable, while the curve for $N = 30$ is widely off and with slope discontinuities in some

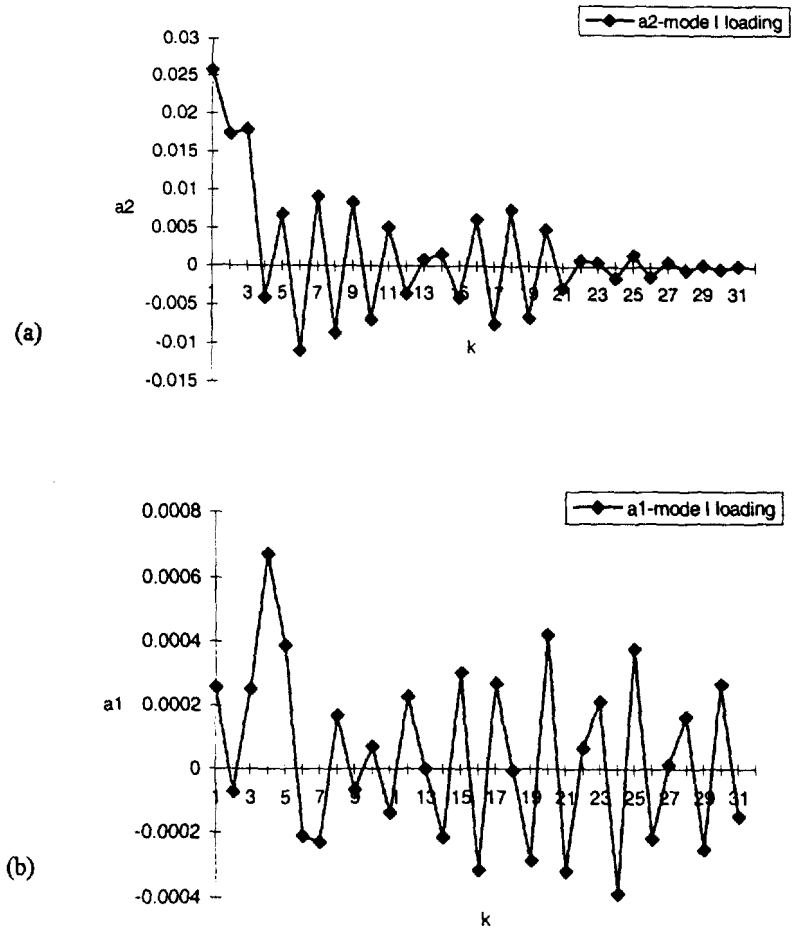

Fig. 8. Poor convergence of the Chebyshev series coefficients, $a_{1,k}$, $a_{2,k}$, for $N = 30$ and mode I loading ($\alpha = 0.8, \beta = 0.3$): (a) beats phenomenon in the dominant Chebyshev series coefficients; (b) no-convergence of the correction Chebyshev series coefficients.

places. Similar behavior is observed in the correction part of the dislocations distribution for mode I loading, $c_1^*(t)$, as shown in Fig. 9(b). These observations were also noted for the other α–β pairs. Hence, it was decided not to discuss the case $N = 30$ any longer.

Convergence of the stress intensity factors

An important result of our calculations is the finding of the local stress intensity factors K_I and K_{II} at the tip of the adhesive-layer crack. The local stress intensity factors are calculated from the Chebyshev series coefficients via eqn (129). The computed local stress intensity factors can be used to check the consistency of the solution. Using the principle of the conservation of the J-integral, the following error formula can be derived:

$$\text{error} = \left| 1 - \frac{K_I^2 + K_{II}^2}{\dfrac{1-\alpha}{1+\alpha}[(K_I^\infty)^2 + (K_{II}^\infty)^2]} \right| \times 100\%. \tag{137}$$

The error estimated with formula (137) is plotted in Fig. 10 for $N = 10$, 20, and 40. Note that, for $N \geqslant 20$, the error becomes small (about 10% for K_I^∞, and about 12% for K_{II}^∞ loading). Comparison of the results obtained with the Singularity Removal Method and the Finite-Part Regularization Technique indicates that both methods give, on average, about the same error.

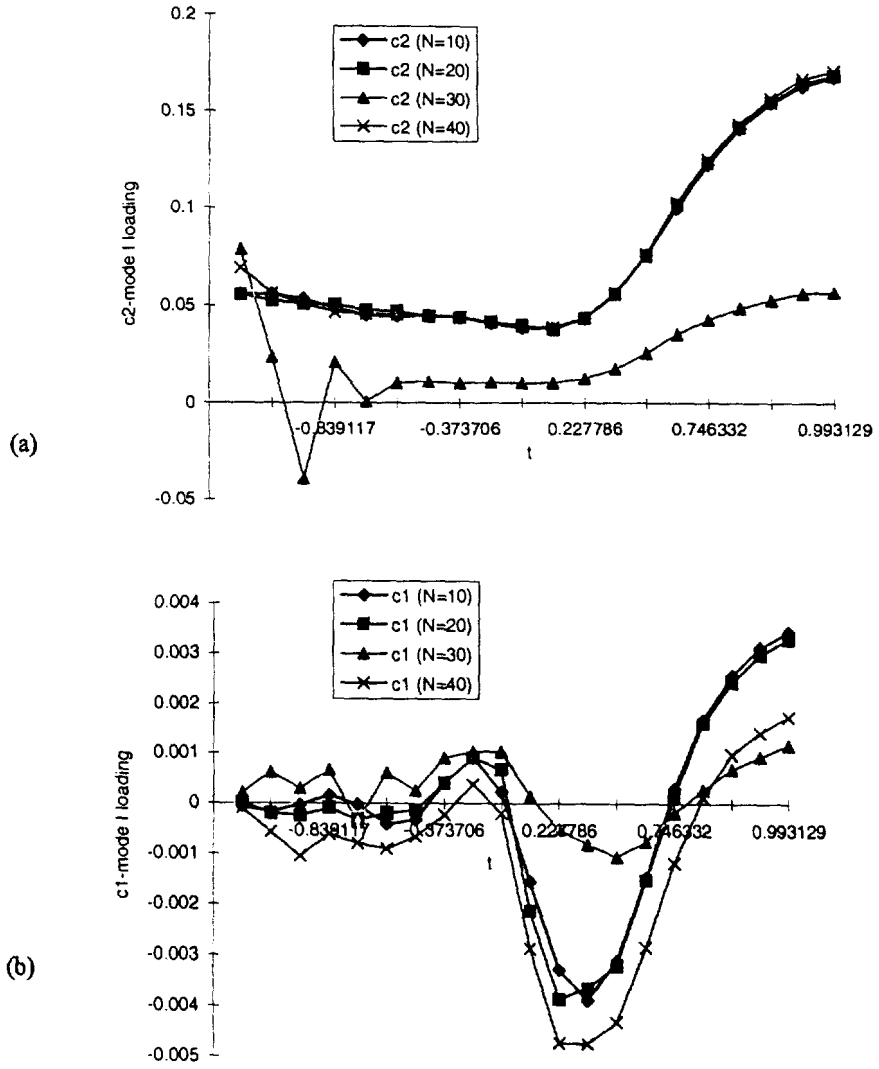

Fig. 9. Convergence of the reconstructed dislocations distribution for mode I loading and $N = 10$, 20, 30, and 40 ($\alpha = 0.8, \beta = 0.3$): (a) the dominant part of the dislocations distributions; (b) the correction part of the dislocations distribution.

Convergence of the c_I and c_{II} *coefficients for the calculation of T-stress*

A convergence study for the c_I and c_{II} coefficients and comparison with the results of Fleck *et al.* (1991) is given in Fig. 11 for $\alpha = 0.9$, $\beta = 0.2$, and $c/H = 0.6$. Good convergence behavior was observed. The discrepancy between our results and those of Fleck *et al.* (1991) is relatively small, and may be attributed to the computational details of the numerical methods used.

CONCLUSIONS

The theoretical developments and the solution algorithm used by Fleck *et al.* (1991) for finding the local stress intensity factors, K_I and K_{II}, and T-stress coefficients, c_I and c_{II}, at the tip of an adhesive layer crack has been studied. The symbolic derivation of the integral equations was reconstructed. To increase the accessibility of new readers to this work, details of the derivations were introduced in several places, as well as some notation modifications.

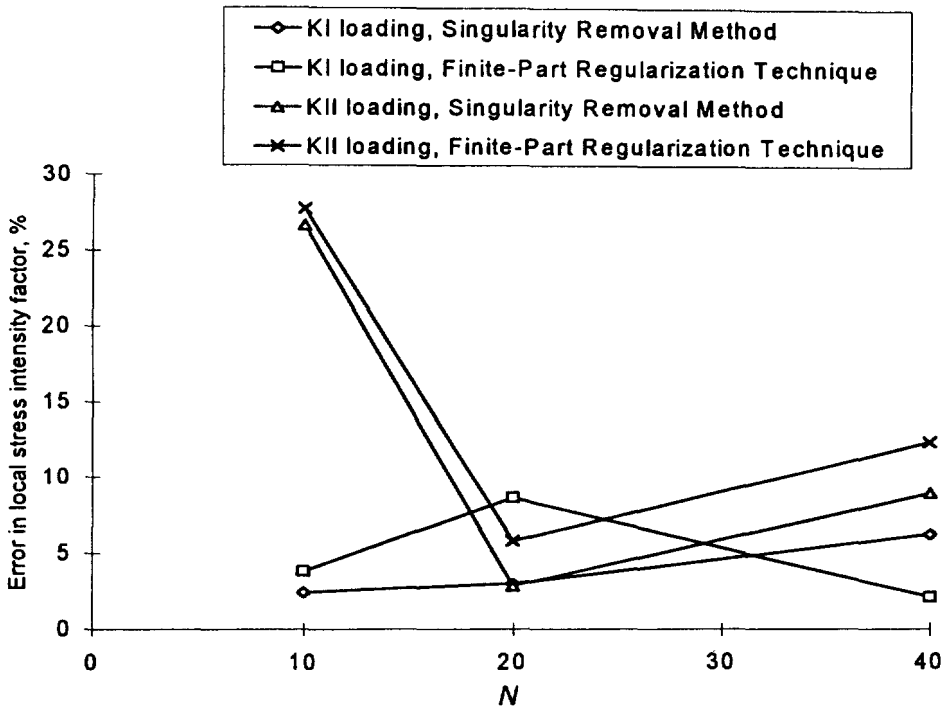

Fig. 10. Percentage error in the evaluation of the local stress intensity factors for $\alpha = 0.8936$, $\beta = 0.2431$ and $N = 10$, 20, and 40.

The numerical part of the solution algorithm was studied extensively. Certain acceleration techniques were used to speed up the computation and increase accuracy, as described in the text. The symbolic solution of the algebraic system in the Fourier domain was used. Particular attention had to be given to the evaluation of the singular integrals determining the coefficients of the linear algebraic system, and special recurrence techniques were used together with the Singularity Removal Method using a change of variables, and the Finite-Part Regularization Technique. Thus, the numerical convergence difficulties at $u = -1$ reported by Giurgiutiu *et al.* (1995) have been successfully overcome. Implementation on a Pentium PC with relatively short computation time was achieved. The convergence of the results with the problem size, N, was examined and was found to be adequate for $N = 40$.

Though the outline of the problem is straightforward, its solution presented some difficulties. Difficulties noted with this method of solution include: convergence of the Chebyshev coefficients and evaluation of certain singular equations. Hence, the use of this solution method requires familiarity with the computational aspects specific to this class of problems.

Acknowledgements—The financial support through the National Science Foundation's Science and Technology Center: High Performance Polymeric Adhesives and Composites at Virginia Tech, Contract DMR 9120004, is gratefully acknowledged. We would also like to acknowledge Professor John W. Hutchinson from Harvard University, Professor Norman Fleck from Cambridge University, England, Professor Zhigang Suo from University of California at Santa Barbara for their extensive help and cooperation. Professors Fleck and Hutchinson also provided some unpublished details of the derivation that served as foundation to our work. Professor Surot Thangjitham, from Virginia Polytechnic Institute and State University, provided collegial interactions. Mr Jeoffrey Graffeo's contributions to this work during his MS studies, though with some convergence difficulties, are also acknowledged.

REFERENCES

***Mathcad 6.0+ Reference Manual, MathSoft, Inc., 201 Broadway, Cambridge, MA, 1995.
Anderson, T. L. (1991) *Fracture Mechanics—Fundamentals and Applications*, CRC Press, Inc., U.S.A.

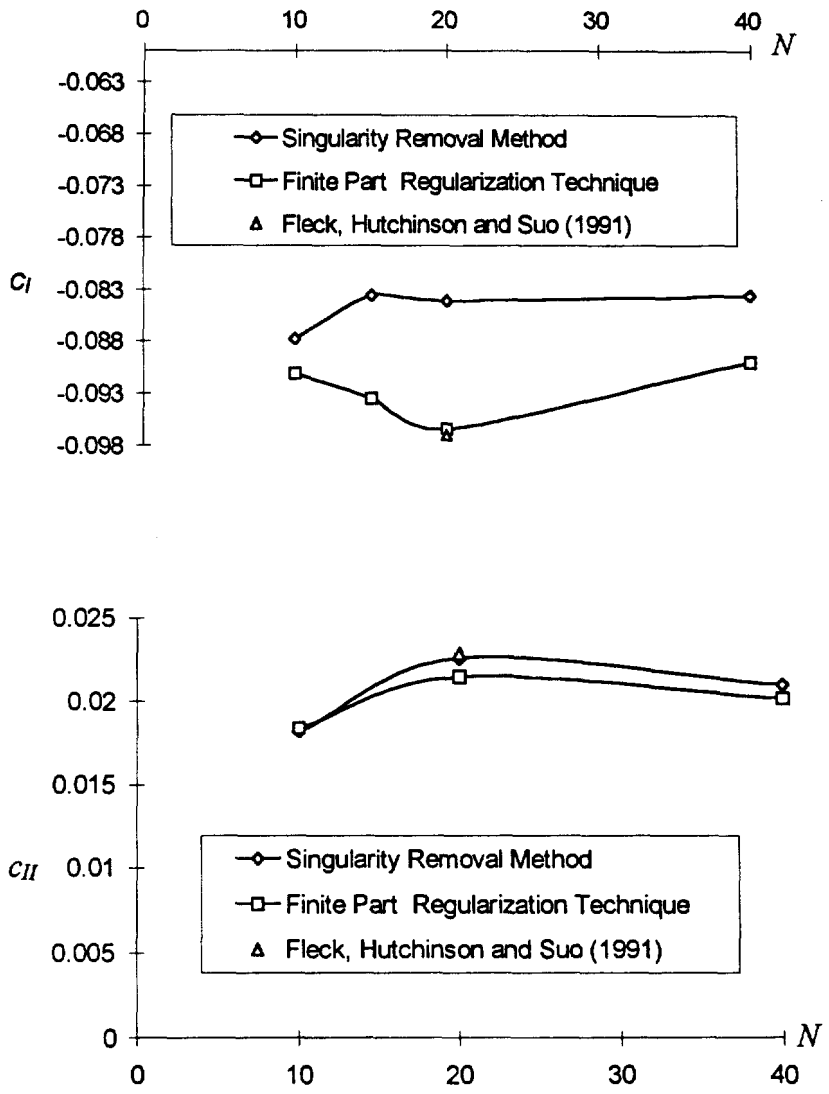

Fig. 11. Variation of the c_I and c_{II} coefficients with the number of collocation points ($\alpha = 0.9, \beta = 0.2, c/H = 0.6$).

Cotterell, B. and Rice, J. R. (1980) Slightly curved or kinked cracks. *International Journal of Fracture* **16,** 155–169.

Dundurs, J. (1968) Elastic interaction of dislocations with inhomogeneities. In *Mathematic Theory of Dislocations*, pp. 70–115. American Society of Mechanical Engineers, New York.

Dundurs, J. (1969) Edge-bonded dissimilar orthogonal elastic wedges under normal and shear loading. *Journal of Applied Mechanics* **36,** 650–652.

Erdogan, F. and Gupta, G. D. (1971) The stress analysis of multi-layered composites with a flaw. *International Journal of Solids and Structures* **7,** 39–61.

Erdogan, F. and Gupta, G. D. (1972) On the numerical solutions of singular equations. *Quarterly of Applied Mathematics* **X,** 525–534.

Fleck, N., Hutchinson, J. W. and Suo, Z. (1991) Crack path selection in a brittle adhesive layer. *International Journal of Solids and Structures* **27**(13), 1683–1703.

Giurgiutiu, V., Graffeo, J., Dillard, D. and Ionita, A. (1995) Computation aspects of using the integral equations method in the analysis of adhesive layer cracks. ASTM 27th National Symposium on Fatigue and Fracture Mechanics, 26–29 June 1995, Williamsburg, VA.

Graffeo, J. (1995) Mathematical modeling of adhesive layer cracks utilizing integral equations. *MS Thesis*, Virginia Polytechnic Institute and State University, E.S.M. Department, Blacksburg VA.

Hutchinson, J. W., Mear, M. E. and Rice, J. R. (1987) Crack paralleling on interface between dissimilar materials. *Journal of Applied Mechanics* **54,** 828–832.

Ionita, A. (1993) A new approach to the two-dimensional problems concerning cracks. In *Proceedings of the 34th AIAA/ASME/ASCE/AHS/ASC Structures, Structural Dynamics, and Materials Convergence*, La Jolla, CA, 19–22 April, paper #AIAA-93-1455-CP, pp. 1319–1325.

Ionita, A., Giurgiutiu, V. and Dillard, D. (1996) Contributions to the numerical solution of the singular integral-equation for the problem of a crack in a layered material system. Virginia Polytechnic Institute and State University, E.S.M. Department, CASS Report, January 1996.

Kecs, W. and Teodorescu, P. P. (1974) *Application of the Theory of Distributions in Mechanics*. Abacus Press, location.

Muskhelisvili, N. I. (1963) *Some Basic Problems of the Mathematical Theory of Elasticity*. P. Noordhoff Ltd., location.

Press, W. H., Teukolsky, S. A., Vetterling, W. T. and Flannery, B. P. (1992) *Numerical Recipes—The Art of Scientific Computing*. Cambridge University Press, UK.

Suo, Z. and Hutchinson, J. W. (1989) Sandwich specimens for measuring interface crack toughness. *Materials Science Engineering* **A107,** 135–143.

Suo, Z. (1989) Singularities interacting with interface cracks. *International Journal of Solids and Structures* **25**(10), 1133–1142.

Westergaard, H. M. (1939) Bearing pressures and cracks. *Journal of Applied Mechanics* **6,** 37–64.

Williams, M. L. (1952) Stress singularities resulting from various boundary conditions in angular corners of plates in extension. *Journal of Applied Mechanics* **19,** 526–528.